



Research article

Finite-time adaptive dynamic surface control for output feedback nonlinear systems with unmodeled dynamics and quantized input delays

Changgui Wu^{1,*} and Liang Zhao²

¹ The City Vocational College of Jiangsu (Nantong), Nantong City, Jiangsu Province, 226006, China

² School of Information Science and Technology, Fudan University, Shanghai, 201203, China

* **Correspondence:** Email: dmyzzm@163.com.

Abstract: We delved into a category of output feedback nonlinear systems that are distinguished by unmodeled dynamics, quantized input delays, and dynamic uncertainties. We introduce a novel finite-time adaptive dynamic surface control scheme developed through the construction of a first-order nonlinear filter. This approach integrates Young's inequality with neural network technologies. Then, to address unmodeled dynamics, the scheme incorporates a dynamic signal and utilizes Radial Basis Function (RBF) neural networks to approximate unknown smooth functions. Furthermore, an auxiliary function is devised to mitigate the impact of input quantization delays on the system's performance. The new controller design is both simple and effective, addressing the "hasingularity" problems typically associated with traditional finite-time controls. Theoretical analyses and simulation outcomes confirm the effectiveness of this approach, guaranteeing that all signals in the system are confined within a finite period.

Keywords: unmodeled dynamics; quantized input time delay; first-order nonlinear filter; finite time stability; dynamic surface control

Mathematics Subject Classification: 93A30, 93C10, 97N40

1. Introduction

With the rapid advancement of science and technology, nonlinear systems are increasingly utilized in various domains, including robot control [1, 2], power systems [3], and communication systems [4]. These systems often display complex dynamic behaviors and significant levels of uncertainty, which pose substantial challenges in control and optimization tasks. Output feedback, a critical method for controlling nonlinear systems, has substantial theoretical and practical value. A nonlinear output feedback system uses the system's output to regulate the input, exhibiting nonlinear characteristics within the internal model itself. Such systems rely on output data for controller design rather than

requiring information from all states. Nonlinear systems, being inherently more complex than linear ones, can exhibit behaviors such as limitations, saturation [5–7], asymmetric responses, and other nonlinear traits. The output feedback mechanism, by capturing system output data in real-time and adjusting accordingly, can achieve system stability and optimization. Theoretically, this mechanism expands the scope of traditional control theory and enhances its applicability across a broader spectrum of fields.

In control engineering and automation, the nonlinearity and uncertainty of systems pose significant challenges to enhancing performance [8, 9]. Traditional linear control theories often fall short in such complex scenarios, failing to achieve the desired control outcomes. As a result, researchers are continually exploring and developing innovative control strategies to overcome these hurdles. The dynamic surface control method, introduced by Swaroop et al. [10], represents a significant advancement over the backstepping approach initially proposed by Kanellakopoulos [11]. This method not only circumvents the over-parameterization issues typical of backstepping designs but also offers a controller structure that is more streamlined, efficient, and intuitive. Both dynamic surface control and backstepping have garnered extensive attention and have been widely applied in designing controllers for nonlinear systems [12–15], providing fresh insights and techniques for improving system performance. Yang and colleagues studied iterative parameter estimation methods for nonlinear feedback systems. They developed a new gradient-based iterative algorithm using negative gradient search and hierarchical identification principles, which significantly improved the accuracy and computational efficiency of parameter estimation [16]. Zhang and his colleagues developed a self-tuning control scheme using a multi-innovation random gradient algorithm. This work is very important and interesting, which ensures the optimal control and stability in discrete-time systems, and these results are proved by supporting simulation [17]. Controlling nonlinear systems remains a pivotal area of academic inquiry, as nonlinearity is an intrinsic characteristic of most real-world systems. Numerous scholars from both domestic and international backgrounds have extensively researched the output feedback control of nonlinear systems, yielding many significant breakthroughs [18, 19]. Despite these advancements, challenges persist, especially when contending with unmodeled dynamics, input quantization, and time delays. Traditional control strategies often fall short of fully ensuring system performance and stability. Unmodeled dynamics can degrade system performance, input quantization, and time delays to complicate control system design. For instance, a novel approach involving dynamic surface control for output feedback nonlinear systems with unmodeled dynamics is explored in [20], where simulations demonstrate its robust dynamic performance. Additionally, in [21], a new controller is crafted using the backstepping design method, effectively mitigating the impacts of unmodeled dynamics and full state constraints. Furthermore, [22] introduces a decentralized adaptive fuzzy output feedback control strategy for stochastic nonlinear systems with dynamic uncertainties, showcasing the evolving complexity of control strategies in response to system challenges. In a recent departure from prior studies, Xu et al. [23] introduced an innovative parameter estimation algorithm leveraging filter identification and model transformation techniques. Their numerical simulations demonstrated that this novel approach achieves more precise parameter estimations compared to several existing correlation identification algorithms, marking a significant advancement in the field of parameter estimation methods.

Input quantization delay is a significant issue in digital control systems, as highlighted in various studies, including those by Xing and Yu [24, 25]. In [26], Li examines the issue of output feedback

resilient control for an uncertain system with two quantized signals under the influence of hybrid network attacks, including denial-of-service and deception attacks. This study is quite interesting, ensures the stability and performance indices of the closed-loop system by designing a cost-preserving resilient controller and solving a set of linear matrix inequalities. A substantial corpus of research, including studies like [27], has explored and analyzed the impacts of input quantization. For instance, the researchers in [28] conducted an in-depth analysis of the stability of strictly feedback nonlinear systems with state quantization, assuming bounded sector regions of the quantizer. Another innovative approach in [24] combined the benefits of lag and uniform quantizers to propose a novel quantizer design that enhances quantization efficiency and offers fresh perspectives for future research. Further, [29] primarily focused on the adaptive event-triggered neural control problem for nonlinear uncertain systems with input delays, introducing an auxiliary system combined with adaptive backstepping techniques to develop a new adaptive time-triggered control strategy. Similarly, [30] investigated the adaptive output feedback control problem for nonlinear systems with input delays and disturbance uncertainties, employing an auxiliary system and backstepping techniques alongside Lyapunov stability theory to offset the effects of input delays. In [31], the adaptive control problem for time-varying delay nonlinear systems with full state constraints was addressed. Researchers constructed suitable Lyapunov-Krasovskii functions to account for uncertainties caused by state and distributed delays. Furthermore, Zhu et al. [32] investigated nonlinear systems that exhibit both input and state delays. They employed state transformation techniques to reformulate the original system into one devoid of input delays, devising an advanced control strategy that amalgamates backstepping, Radial Basis Function (RBF) neural networks, and adaptive control approaches. Their research contributes innovative strategies and methodologies for addressing the challenges associated with delays in intricate dynamic systems.

The adoption of finite-time control strategies has surged due to their ability to achieve rapid and accurate control in various applications. These methods, which are the focus of contemporary research like that of Fang et al. [33], provide efficient and effective solutions for dynamic system regulation within a fixed time frame, enhancing both system performance and stability. This approach is distinguished by its ability to bring system states to equilibrium within a finite timeframe, after which they remain stable [34]. The foundational framework for finite-time stability, which utilizes Lyapunov theory and homogeneous systems theory, was first established in [35]. Additionally, [36] explored a class of strict-feedback nonlinear systems with known control gains and virtual coefficients, introducing a finite-time adaptive control strategy via the backstepping design method. While this strategy marks a significant advancement in control efficiency, it overlooks the potential impacts of input quantization delays on system performance, a critical consideration for practical applications. Furthermore, in [37], researchers applied dynamic surface control techniques and incorporated a novel first-order filter into their designs. However, the use of a sign function in the virtual controller's design rendered the control law non-differentiable, leading to theoretical inaccuracies and, ultimately, algorithm failure. Beyond ensuring that system states achieve desired values or stability within a finite timeframe, finite-time control strategies also potentially enhance the system's resilience against external disturbances.

To tackle the challenges mentioned above, this study introduces a novel finite-time dynamic surface control strategy designed for managing output feedback systems plagued by unmodeled dynamics, quantized input delays, and external disturbances. The primary contributions of this research include:

(1) For output feedback systems affected by unmodeled dynamics and quantized input delays, we introduce a first-order auxiliary system to generate dynamic signals that tackle unmodeled dynamics, and the system replaces traditional first-order linear low-pass filters with first-order nonlinear filters. This research innovates by integrating input quantization and delays, through the design of an auxiliary function that compensates for delays caused by quantization. Furthermore, neural networks are employed to approximate unknown functions. By integrating these with dynamic surface technology, a new finite-time adaptive dynamic surface control strategy is proposed.

(2) The virtual control law designed in this paper is characterized by its continuous differentiability, which effectively circumvents the potential singularity issues associated with control derivatives noted in [38], and mitigates discontinuity issues related to neural network approximation functions. Additionally, unlike the virtual control strategies that utilize sign functions as detailed in [37, 39], the proposed control scheme ensures the differentiability of the virtual control law. This introduction effectively provides an overview of the research background, addresses the key challenges, and highlights the significant contributions of this study, laying a solid groundwork for a detailed exploration of the article's content.

The remainder of this paper is structured as follows: In Section 2 introduce the problem, outline useful lemmas, and detail necessary assumptions. In Section 3, we describe the development of an RBF-based adaptive controller and establishes its stability through the design of Lyapunov functions. In Section 4, we demonstrate the effectiveness of the proposed control method through numerical simulations using MATLAB. Finally, in Section 5 we present the conclusions of this study, encapsulating the findings and implications.

2. Problem statement and preliminaries

2.1. Dynamics of nonlinear systems

Consider the following type of output feedback nonlinear system, characterized by unique unmodeled dynamics and quantized input time delays:

$$\left\{ \begin{array}{l} \dot{\zeta} = Q(\zeta, y, t) \\ \dot{x}_1 = x_2 + f_1(y) + D_1(\zeta, y, t) \\ \vdots \\ \dot{x}_{s-1} = x_s + f_{s-1}(y) + D_{s-1}(\zeta, y, t) \\ \dot{x}_s = x_{s+1} + f_s(y) + D_s(\zeta, y, t) + b_m q(v(t - \tau)) \\ \vdots \\ \dot{x}_n = f_n(y) + D_n(\zeta, y, t) + b_0 q(v(t - \tau)) \\ y = x_1 \end{array} \right. \quad (2.1)$$

where $x_i (i = 1, 2, \dots, n)$ represent the state variables of the system, $f_i(y)$ denotes unknown smooth nonlinear functions, $\zeta \in \mathbb{R}^{n_0}$ encapsulates the unmodeled dynamics, $y \in \mathbb{R}$ is the system output, and $v \in \mathbb{R}$ is the system input. The term $D_i(\zeta, y, t)$ describes unknown nonlinear disturbances. $B(s) = b_m s^m + \dots + b_1 s + b_0$ is a Hurwitz polynomial, with b_m, \dots, b_0 as unknown coefficients. The expression $q(v(t - \tau))$ represents the quantized form of the input signal, where τ is a known positive constant indicating the input delay.

2.2. Some useful lemmas and assumptions

Assumption 1. [20] The desired trajectory vector $x_d = [y_d, \dot{y}_d, \ddot{y}_d]^T \in \Omega_d$ belongs to the set Ω_d , where Ω_d is defined as $\Omega_d = \{x_d : y_d^2 + \dot{y}_d^2 + \ddot{y}_d^2 \leq B_0\}$. Additionally, the absolute value $|y_d|$ does not exceed B_1 . Here, B_0 and B_1 are known positive constants.

Assumption 2. [19] For the unknown disturbances $D_i(\zeta, y, t)$, where $i = 1, 2, \dots, n$, there exist unknown non-negative continuous functions $\Delta_{i1}(\cdot)$ and unknown non-negative continuous monotonically increasing functions $\Delta_{i2}(\cdot)$ such that the absolute value of the disturbances is bounded by the sum of these two functions:

$$|D_i(\zeta, y, t)| \leq \Delta_{i1}(|y|) + \Delta_{i2}(\|\zeta\|), \quad (2.2)$$

where $|\cdot|$ denotes the Euclidean norm.

Assumption 3. [40] For the system described by $\dot{\zeta} = Q(\zeta, y, t)$, the unmodeled dynamics ζ are exponentially input-to-state stable.

Assumption 4. [20] There is a known positive constant b_{\max} that satisfies the inequality $0 < |b_m| \leq b_{\max}$.

Lemma 1. [40] Suppose that $V_0(\zeta)$ is a Lyapunov function for the system $\dot{\zeta} = Q(\zeta, y, t)$ that is exponentially input-to-state practically stable. Then, for any constant $\bar{c}_f \in (0, c)$, initial time $t_0 > 0$, initial state $\zeta_0 = \zeta(t_0)$, initial radius $r_0 > 0$, and any $\bar{\Lambda}(|y|) \geq \Lambda(|y|)$, there exists a finite time $T_0 = \max\left\{0, \frac{\ln[V_0(\zeta_0)/r_0]}{c-\bar{c}_f}\right\} \geq 0$ and a non-negative function $D(t_0, t)$, such that the dynamic signal satisfies:

$$\dot{r} = -\bar{c}_f r + \bar{\Lambda}(|y|) + d. \quad (2.3)$$

For $t \geq t_0 + T_0$, $D(t_0, t) = 0$ and $V_0(\zeta) \leq r(t) + D(t_0, t)$ hold. Without loss of generality, it can be assumed that $\bar{\Lambda}(|y|) = \Lambda(|y|)$.

Lemma 2. [41] Consider the nonlinear system $\dot{x} = f(x)$. If there exists a smooth positive-definite function $V(x)$ and scalar parameters $\alpha > 0, \beta > 0, \frac{1}{2} < q < 1, 0 < C < \infty$, and $0 < \nu < 1$ that satisfy:

$$\dot{V}(x) \leq -\alpha V(x) - \beta V^q(x) + C, \quad (2.4)$$

then the system is practically finite-time stable, with a settling time $T_0 \leq \frac{1}{\alpha(1-q)} \ln \frac{\alpha V^{1-q}(x_0) + \nu\beta}{\alpha \left(\frac{C}{(1-q)\beta}\right)^{\frac{1-q}{q}} + \nu\beta}$.

Lemma 3. [41] For any positive real numbers η_1, \dots, η_N and a constant m between 0 and 1 ($0 \leq m < 1$), the inequality $\sum_{i=1}^N \eta_i^m \geq \left(\sum_{i=1}^N \eta_i\right)^m$ holds.

Lemma 4. [42] Let a and b be non-negative real numbers, and let p and q be positive real numbers such that $\frac{1}{p} + \frac{1}{q} = 1$ (where $p, q > 1$). Then Young's inequality states that:

$$ab \leq \frac{a^p}{p} + \frac{b^q}{q}. \quad (2.5)$$

Lemma 5. [20] For any continuous real function $f(x, y)$, there exist two smooth non-negative scalar functions $\varphi_0(x)$ and $\vartheta_0(y)$ such that the inequality

$$|f(x, y)| \leq \varphi_0(x) + \vartheta_0(y) \quad (2.6)$$

holds, where x is in R^m and y is in R^n .

2.3. Control objective

Our objective is to design a controller v and a quantizer $q(v)$ that enable the system output y to accurately follow a predefined desired trajectory y_d . The approach aims to ensure that all signals in the closed-loop system remain bounded within a finite timeframe and to minimize the tracking error. We employ a first-order nonlinear filter and a dynamic surface control strategy to effectively address uncertainties caused by unmodeled dynamics and input delays. Additionally, we seek to improve the system's handling of quantized inputs, thereby enhancing the overall response speed and stability of the system.

3. Design of adaptive controller and stability proof

3.1. RBF neural network

Remark 1. The Radial Basis Function (RBF) neural network, a specialized type of artificial neural network, is characterized by its use of radial basis functions as activation functions in the hidden layer, as detailed in recent research [43,44]. This network structure typically includes an input layer, a hidden layer where neurons utilize functions like the Gaussian for non-linear transformations, and an output layer. RBF networks are particularly valued for their ability to universally approximate any continuous function, making them highly effective in various function approximation tasks.

Define a compact set $\Pi_y = \{y \mid \|y\| \leq M_y\} \subset R^{L_i}$, where $M_y > 0$ is a predetermined design constant. If a RBF neural network $\Theta_i^* \varphi_i(y)$ is used to approximate an unknown continuous function $f_i(y)$ on the compact set Π_{Z_i} , then

$$f_i(y) = \Theta_i^{*T} \varphi_i(y) + \delta_i(y), \quad (3.1)$$

where $\delta_i(y)$ represents the approximation error, $\varphi_i(y)$ is a vector composed of multiple RBFs, specifically $\varphi_i(y) = [\varphi_{i1}(y), \dots, \varphi_{iM_i}(y)]^T \in R^{M_i}$. Each radial basis function $\varphi_{ij}(y)$ is defined as a Gaussian function, defined by:

$$\varphi_{ij}(y) = \exp \left[-\frac{(y - \mu_{ij})^2}{b_{ij}^2} \right], \quad (3.2)$$

where μ_{ij} and b_{ij} represent the center and width parameters of the Gaussian functions, respectively, for $1 \leq i \leq n$ and $1 \leq j \leq M_i$. The term M_i indicates the number of nodes in the i -th neuron. Additionally, the ideal weights are defined as follows:

$$\Theta_i^* = \arg \min_{\Theta_i \in R^{M_i}} \left[\sup_{y \in \Omega_y} |\Theta_i^T \varphi_i(y) - f_i(y)| \right]. \quad (3.3)$$

According to the above formula, Eq (2.1) can be rewritten as

$$\begin{cases} \dot{\zeta} = Q(\zeta, y, t) \\ \dot{x} = Ax + F^T(y, q(v(t - \tau)))\Theta + \delta(y) + D(\zeta, y, t) \\ y = e_1^T x \end{cases}, \quad (3.4)$$

where,

$$\phi^T(y) = \begin{bmatrix} \varphi_1^T(y) & 0 & 0 \\ 0 & \ddots & 0 \\ 0 & 0 & \varphi_n^T(y) \end{bmatrix}, \quad \Theta_f = \begin{bmatrix} \Theta_1^* \\ \vdots \\ \Theta_n^* \end{bmatrix}, \quad \delta(y) = \begin{bmatrix} \delta_1(y) \\ \vdots \\ \delta_n(y) \end{bmatrix}, \quad A = \begin{bmatrix} 0 & I_{n-1} \\ 0 & 0 \end{bmatrix},$$

$$F^T \left(y, q(v(t-\tau)) \right) = \begin{bmatrix} 0 \\ (s-1) \times (m+1) \\ I_{m+1} \end{bmatrix} q(v(t-\tau)), \phi^T(y), \quad \Theta = \begin{bmatrix} b \\ \Theta_f \end{bmatrix} \in R^{(m+1+N)},$$

$$s = n - m, N = \sum_{i=1}^n M_i, \quad x = \begin{bmatrix} x_1 \\ \vdots \\ x_n \end{bmatrix}, \quad D(\zeta, y, t) = \begin{bmatrix} D_1(\zeta, y, t) \\ \vdots \\ D_n(\zeta, y, t) \end{bmatrix}, \quad b = \begin{bmatrix} b_m \\ \vdots \\ b_0 \end{bmatrix}, \quad e_1 = \begin{bmatrix} 1 \\ 0 \\ \vdots \\ 0 \end{bmatrix}.$$

Since only the system output y is measurable and the other states are unobservable, we have designed the following filter to reconstruct the states of the system.

$$\begin{cases} \dot{\zeta} = A_0 \zeta + Ly, & \zeta \in R^n \\ \dot{\Omega}^T = A_0 \Omega^T + F^T(y, q(v(t-\tau))), & \Omega^T \in R^{n \times (m+1+N)}. \end{cases} \quad (3.5)$$

Let $L = [l_1, \dots, l_n]^T$ and $A_0 = A - Le_1^T$, where both are Hurwitz matrices that satisfy the equation $PA_0 + A_0^T P = -hI$. Here, P is a positive definite symmetric matrix ($P = P^T > 0$), and $h > 0$ is a design constant.

Define the matrix $\Omega^T = [v_m, \dots, v_0, \Xi]$, size $R^{n \times (m+1+N)}$, and vectors $v_j (j = 0, 1, \dots, m)$ follow the equation

$$v_j = A_0^j \lambda, \quad (3.6)$$

$$A_0^j e_n = e_{n-j}, \quad (3.7)$$

$$\dot{v}_j = A_0 v_j + e_{n-j} q(v(t-\tau)), \quad (3.8)$$

where A_0^j represents the j -th power of the matrix A_0 . In accordance with Eq (3.4), the matrix Ξ must meet the following conditions:

$$\dot{\Xi} = A_0 \Xi + \phi^T(y). \quad (3.9)$$

The following equation can be obtained from Eq (3.6):

$$v_{i,j} = [*, \dots, *, 1] \begin{bmatrix} \lambda_1 \\ \vdots \\ \lambda_{i+j} \end{bmatrix}, \quad (3.10)$$

where $i = 0, 1, \dots, m, j = 1, 2, \dots, n, \lambda_k = 0, k > n$

Design the following state observer:

$$\dot{\hat{x}} = \Upsilon + \Omega^T \Theta. \quad (3.11)$$

The observer error is defined as:

$$\varepsilon = x - \hat{x}. \quad (3.12)$$

Taking the derivative of this error gives:

$$\dot{\varepsilon} = A_0\varepsilon + \delta(y) + D(\zeta, y, t). \quad (3.13)$$

In summary, the general form of the filter is expressed as follows:

$$\begin{cases} \dot{\Upsilon} = A_0\Upsilon + Ly, \Upsilon \in R^n \\ \dot{\Xi} = A_0\Xi + \phi^T(y), \Xi \in R^{n \times N} \\ \dot{\lambda} = A_0\lambda + e_n q(v(t - \tau)), \lambda \in R^n \end{cases}. \quad (3.14)$$

Based on the above analysis, the expression for the system state x_2 can be derived as follows:

$$\begin{aligned} x_2 &= \hat{x}_2 + \varepsilon_2 \\ &= \Upsilon_2 + \Omega_2^T \Theta + \varepsilon_2 \\ &= b_m v_{m,2} + \zeta_2 + [0, v_{m-1,2}, \dots, v_{0,2}, \Xi_{(2)}] \Theta + \varepsilon_2, \end{aligned} \quad (3.15)$$

where $\Omega_{(2)}^T$ denotes the second row of the matrix Ω^T , $\Xi_{(2)}$ denotes the second row of the matrix Ξ , Υ_2 is the second element of the column vector Υ , and ε_2 is the second element of the column vector ε . Using Eqs (3.4) and (3.15), we obtain the following:

$$\dot{y} = b_m v_{m,2} + \Upsilon_2 + \varpi^T \Theta + \varepsilon_2 + \delta_1(y) + D_1(\zeta, y, t). \quad (3.16)$$

Here, $\varpi^T = [0, v_{m-1,2}, \dots, v_{0,2}, \Xi_{(2)} + \phi_{(1)}^T]$, where $\phi_{(1)}^T$ represents the first row of the matrix ϕ^T . By combining Eqs (3.6) and (3.8), the following description of a system of order ρ can be derived:

$$\begin{cases} \dot{y} = b_m v_{m,2} + \Upsilon_2 + \varpi^T \Theta + \varepsilon_2 + \delta_1(y) + D_1(\zeta, y, t) \\ \dot{v}_{m,i} = v_{m,i+1} - l_i v_{m,1}, i = 2, \dots, s-1 \\ \dot{v}_{m,s} = q(v(t - \tau)) + v_{m,s+1} - l_s v_{m,1} \end{cases}. \quad (3.17)$$

3.2. Design of quantizer

Remark 2. The quantizer presented in this study combines features from both hysteresis and uniform quantizers to enhance system performance, as noted by Linde in his seminal work [45]. Hysteresis quantizers, known for their ability to reduce signal chattering through variable transition thresholds, limit frequent switching, enhancing signal stability. Uniform quantizers, on the other hand, keep quantization errors within a predictable upper bound throughout the operation, crucial for maintaining system reliability. The integration of these two quantizer types in the new design not only improves the system's dynamic responses but also stabilizes the quantization error, thereby increasing the overall system efficiency and reliability as further explored by Sun [46].

In this section, the new quantizer is described as follows:

$$q(v) = \begin{cases} q_h(v_{th}) + \text{Int} \left[\frac{v-v_{th}}{\bar{v}} + \kappa(v_{th}) \right] \bar{v}, & |v| \geq v_{th}, \\ q_h(v), & |v| < v_{th}, \end{cases} \quad (3.18)$$

where,

$$q_h(v) = \begin{cases} v_i \operatorname{sgn}(v), & \frac{v_i}{1+\delta} < |v| < v_i, \dot{v} < 0, \text{ or} \\ v_i(1 + \delta) \operatorname{sgn}(v), & v_i < |v| \leq \frac{v_i}{1-\delta}, \dot{v} > 0 \\ 0, & \frac{v_i}{1-\delta} < |v| < \frac{v_i(1+\delta)}{1-\delta}, \dot{v} > 0 \\ q_h(v(t^-)), & 0 \leq |v| < \frac{v_{\min}}{1+\delta}, \text{ or} \\ \dot{v} = 0 & \frac{v_{\min}}{1+\delta} < |v| \leq v_{\min}, \dot{v} > 0 \end{cases}, \quad (3.19)$$

$$\kappa(v_{th}) = \begin{cases} 1, & q_h(v_{th}) < v_{th} \\ 0, & q_h(v_{th}) \geq v_{th} \end{cases}, \quad (3.20)$$

where, each v_i is defined as $p^{1-i}v_{\min}$ where $i = 1, 2, \dots$ and $v_{\min} > 0$ is a positive constant. The parameter $0 < p < 1$ is crucial as it regulates the dead zone size in the function $q_h(u)$, with $\delta = \frac{1-p}{1+p}$ reflecting the quantization density. The function $q_h(v)$ assigns values within the set $U = 0, \pm v_i, \pm v_i(1 + \delta)$. $\operatorname{Int}[a]$ is the greatest integer less than or equal to a . The term $\bar{v} \geq |q_h(v_{th}) - v_{th}|$ represents a design parameter that controls the quantization density for the uniform quantizer. v_{th} , another positive design constant, determines the switching threshold for the hysteresis and uniform quantizers. This framework leads to the derivation of the expression for quantization error, enhancing our understanding of quantizer behavior and error dynamics

$$|\Delta_q| \leq \begin{cases} \bar{v}, & |v| \geq v_{th} \\ \delta v_{th} + (1 - \delta)v_{\min}, & |v| < v_{th} \end{cases}. \quad (3.21)$$

Clearly, the quantization error Δ_q of the new quantizer is bounded for any v , meaning there exists a positive constant d such that $|\Delta_q| \leq d$, where d is defined as $d = \max\{\bar{v}, \delta v_{th} + (1 - \delta)v_{\min}\}$. Based on the definition $\Delta_q(v) = q(v) - v$, we can derive:

$$q(v) = v + \Delta_q(v). \quad (3.22)$$

3.3. Design of controller

Develop an auxiliary function to mitigate the effects of quantization delay. This function aims to refine and enhance the data processing workflow, effectively minimizing or removing the delays associated with data quantization and processing.

The auxiliary function is described as follows:

$$\begin{cases} \dot{\lambda}_i = \lambda_{i+1} - c_i \lambda_i (i = 1, \dots, s-1) \\ \dot{\lambda}_s = -c_s \lambda_s + q(v(t - \tau)) - q(v) \end{cases}. \quad (3.23)$$

To design an adaptive controller, the following coordinate transformation is performed:

$$\begin{cases} z_1 = y - y_d - \lambda_1 \\ z_i = v_{m,i} - \omega_i - \lambda_i \end{cases}, \quad (3.24)$$

where ω_i is the output of a first-order filter with α_{i-1} as its input, for $i = 2, \dots, s$.

To simplify the design process, several notations are defined:

$$\begin{aligned} \text{sig}(\cdot)^m &= |\cdot|^m \text{sgn}(\cdot), \quad \theta_i = \|W_{hi}^*\|^2, \quad \bar{z}_i = [z_1, \dots, z_i]^T, \quad \bar{y}_j = [y_2, \dots, y_j]^T, \\ \bar{\hat{\theta}}_i &= [\hat{\theta}_1, \dots, \hat{\theta}_i]^T, \quad 1 \leq i \leq s, 2 \leq j \leq s, \quad \tilde{\theta}_i = \theta_i - \hat{\theta}_i, \quad \tilde{b}_m = b_m - \hat{b}_m, \\ \tilde{\Theta} &= \Theta - \hat{\Theta}, \quad V_1 = V_\varepsilon + V_{z1} + \frac{r}{\lambda_0}. \end{aligned}$$

In the adaptive controller design, specific variables are designated as follows: $\hat{\theta}_i$, \hat{b}_m , and $\hat{\Theta}$ are the time-dependent estimates of θ_i , b_m , and Θ , respectively, at time t . Additionally, for each corresponding index j , y_j is defined as $\omega_j - \alpha_{j-1}$.

The design includes the definition of a Lyapunov function candidate:

$$V_\varepsilon = \varepsilon^T p \varepsilon. \quad (3.25)$$

Here, V_ε is a function intended to demonstrate the stability of the adaptive control system, where ε is a vector of error terms, and p is a positive definite matrix.

The time derivative of V_ε is given by:

$$\begin{aligned} \dot{V}_\varepsilon &= \dot{\varepsilon}^T p \varepsilon + \varepsilon^T p \dot{\varepsilon} \\ &= \varepsilon^T (pA_0 + A_0^T p) \varepsilon + 2\varepsilon^T p \delta + 2\varepsilon^T p D \\ &\leq -(h-2)\varepsilon^T \varepsilon + \|p\|^2 \|\delta\|^2 + \|p\|^2 \|D\|^2, \end{aligned} \quad (3.26)$$

where A_0 denotes the nominal system matrix, while δ signifies the uncertainties or disturbances impacting the system, and D captures modeling inaccuracies or other deviations. The expression $pA_0 + A_0^T p$ is associated with the Lyapunov equation, which is integral to determining the stability of the system, emphasizing the system's ability to return to equilibrium in the face of perturbations.

Based on Assumption 2 and Lemma 4, we can obtain

$$\begin{aligned} \dot{V}_\varepsilon &\leq -(h-2)\varepsilon^T \varepsilon + \sum_{j=1}^n \|p\|^2 \|\delta_j\|^2 + \sum_{j=1}^n \|p\|^2 (\Delta_{j1}(|y|) + \Delta_{j2}(\|\xi\|))^2 \\ &\leq -(h-2)\varepsilon^T \varepsilon + \sum_{j=1}^n \|p\|^2 \|\delta_j\|^2 + 2 \sum_{j=1}^n \|p\|^2 (\Delta_{j1}^2(|y|) + \Delta_{j2}^2(\|\xi\|)) \\ &\leq -(h-2)\varepsilon^T \varepsilon + \sum_{j=1}^n \|p\|^2 \|\delta_j\|^2 + 2 \sum_{j=1}^n \|p\|^2 \Delta_{j1}^2(|y|) \\ &\quad + \|p\|^2 \varphi_0(r) + \|p\|^2 \vartheta_0(D(t_0, t)) \\ &\leq -(h-2)\varepsilon^T \varepsilon + \sum_{j=1}^n \|p\|^2 \|\delta_j\|^2 + 2 \sum_{j=1}^n \|p\|^2 \Delta_{j1}^2(|y|) + \|p\|^2 \varphi_0(r) + \|p\|^2 \vartheta_0^*, \end{aligned} \quad (3.27)$$

where the functions $\varphi_0(\cdot)$ and $\vartheta_0(\cdot)$ are unknown continuous functions that are central to the system's dynamic behavior. Hence, there exists a constant ϑ_0^* such that the inequality:

$$\vartheta_0(D(t_0, t)) \leq \vartheta_0^*. \quad (3.28)$$

Step 1. Defining the first dynamic surface

$$z_1 = y - y_d - \lambda_1, \quad (3.29)$$

where z_1 represents the error between the actual output y and the desired output y_d .

The time derivative of z_1 is:

$$\begin{aligned} \dot{z}_1 &= \dot{y} - \dot{y}_d - \dot{\lambda}_1 \\ &= b_m(z_2 + y_2 + \alpha_1 + \lambda_2) + \zeta_2 + \varpi^T \Theta + \varepsilon_2 + \delta_1 + D_1 - \dot{y}_d - \lambda_2 + c\lambda_1. \end{aligned} \quad (3.30)$$

Take Lyapunov function

$$V_{z_1} = \frac{1}{2}z_1^2 + \frac{1}{2}\tilde{\theta}_1^2 + \frac{1}{2}\tilde{b}_m^2 + \frac{1}{2}\tilde{\Theta}^2. \quad (3.31)$$

The derivative of V_{z_1} about t is obtained:

$$\begin{aligned} \dot{V}_{z_1} &= z_1\dot{z}_1 - \tilde{\theta}_1\dot{\tilde{\theta}}_1 - \tilde{b}_m\dot{\tilde{b}}_m - \tilde{\Theta}\dot{\tilde{\Theta}} \\ &= z_1 \left[b_m(z_2 + y_2 + \alpha_1 + \lambda_2) + \zeta_2 + w^T \Theta + \varepsilon_2 + \delta_1 + D_1 - \dot{y}_d - \lambda_2 + c\lambda_1 \right] \\ &\quad - \tilde{\theta}_1\dot{\tilde{\theta}}_1 - \tilde{b}_m\dot{\tilde{b}}_m - \tilde{\Theta}\dot{\tilde{\Theta}}. \end{aligned} \quad (3.32)$$

Using Young's inequality and based on Assumption 4, we derive the following:

$$b_m z_1 z_2 \leq \frac{b_{\max}^2}{4} z_1^2 + z_2^2. \quad (3.33)$$

$$b_m z_1 y_2 \leq \frac{b_{\max}^2}{4} z_1^2 + y_2^2. \quad (3.34)$$

$$b_m z_1 \lambda_2 \leq \frac{z_1^2 \lambda_2^2}{4} + b_{\max}^2. \quad (3.35)$$

$$-\lambda_2 z_1 \leq 1 + \frac{z_1^2 \lambda_2^2}{4}. \quad (3.36)$$

$$\begin{aligned} z_1 D_1 &\leq z_1 [\Delta_{11}(|y|) + \Delta_{12}(\|\zeta\|)] \\ &\leq z_1^2 [\Delta_{11}(|y|) + \Delta_{12} \circ \bar{\alpha}_1(r + D_0)]^2 + \frac{1}{4}. \end{aligned} \quad (3.37)$$

The Eq (3.32) can be transformed into:

$$\begin{aligned} \dot{V}_{z_1} &\leq z_1 \left[b_m \alpha_1 + \zeta_2 + \varpi^T \Theta + \varepsilon_2 + \delta_1 - \dot{y}_d + c\lambda_1 + \frac{b_{\max}^2}{2} z_1 + \frac{1}{2} \lambda_2^2 z_1 \right. \\ &\quad \left. + z_1 [\Delta_{11}(|y|) + \Delta_{12} \circ \bar{\alpha}_1(r + D_0)]^2 \right] + \frac{5}{4} + b_{\max}^2 + y_2^2 + z_2^2 - \tilde{\theta}_1\dot{\tilde{\theta}}_1 - \tilde{b}_m\dot{\tilde{b}}_m - \tilde{\Theta}\dot{\tilde{\Theta}}. \end{aligned} \quad (3.38)$$

Let

$$H_1(X_1) = -\dot{y}_d + c\lambda_1 + \frac{1}{2}\lambda_2^2 z_1 + z_1 [\Delta_{11}(|y|) + \Delta_{12} \circ \bar{\alpha}_1(r + D_0)]^2 + |z_1|^{2q-1}, \quad (3.39)$$

where $X_1 = [z_1, y_d, \dot{y}_d, \lambda_1, \lambda_2, r]^T$.

Then

$$\begin{aligned} \dot{V}_{z_1} \leq & z_1 \left[b_m \alpha_1 + \zeta_2 + \varpi^T \Theta + \varepsilon_2 + \delta_1 + \frac{b_{\max}^2}{2} z_1 + W_{h1}^{*T} \psi_1(X_1) + B_1(X_1) \right] \\ & + \frac{5}{4} + b_{\max}^2 + y_2^2 + z_2^2 - \tilde{\theta}_1 \hat{\theta}_1 - \tilde{b}_m \hat{b}_m - \tilde{\Theta} \hat{\Theta} - |z_1|^{2q}. \end{aligned} \quad (3.40)$$

According to Young's inequality, we can see that:

$$z_1 W_{h1}^{*T} \psi_1(X_1) \leq \frac{\|\psi_1(X_1)\|^2 z_1^2 \theta_1}{2a_1^2} + \frac{a_1^2}{2}, \quad (3.41)$$

where a_1 is a positive constant which is strategically chosen as part of the design of the control system. Given the importance of this design constant, Eq (3.40) can then be transformed as follows:

$$\begin{aligned} \dot{V}_{z_1} \leq & z_1 \left[b_m \alpha_1 + \Upsilon_2 + w^T \Theta + \varepsilon_2 + \delta_1 + \frac{b_{\max}^2}{2} z_1 + \frac{\|\psi_1(X_1)\|^2 z_1 \theta_1}{2a_1^2} + B_1(X_1) \right] \\ & + \frac{5}{4} + b_{\max}^2 + y_2^2 + z_2^2 - \tilde{\theta}_1 \hat{\theta}_1 - \tilde{b}_m \hat{b}_m - \tilde{\Theta} \hat{\Theta} - |z_1|^{2q} + \frac{a_1^2}{2}. \end{aligned} \quad (3.42)$$

A virtual control law is designed as follows:

$$\alpha_1 = -\frac{\hat{b}_m}{\hat{b}_m^2 + \beta} \left((k_1 + 3) z_1 + \Upsilon_2 + \varpi^T \hat{\Theta} + \frac{\|\psi_1(X_1)\|^2 z_1 \hat{\theta}_1}{2a_1^2} \right). \quad (3.43)$$

The adaptive law is designed as follows:

$$\dot{\hat{\theta}} = \frac{\|\psi_1(X_1)\|^2 z_1^2}{2a_1^2} - \sigma_1 \hat{\theta}_1, \quad (3.44)$$

$$\dot{\hat{b}}_m = z_1 \alpha_1 - \gamma_1 \hat{b}_m, \quad (3.45)$$

$$\dot{\hat{\Theta}} = \varpi z_1 - \gamma_2 \hat{\Theta}, \quad (3.46)$$

where the constants k_1 , σ_1 , β , γ_1 , and γ_2 are all set to positive values.

Substituting the Eqs (3.43)–(3.46) into the Eq (3.42), we get:

$$\begin{aligned} \dot{V}_{z_1} \leq & z_1 B_1(X_1) - \left(k_1 - \frac{b_{\max}^2}{2} \right) z_1^2 + z_1 \varepsilon_1 + z_1 \delta_1 - \frac{z_1 \beta}{\hat{b}_m^2 + \beta} \left(-(k_1 + 3) z_1 - \Upsilon_2 \right. \\ & \left. - \varpi^T \hat{\Theta} - \frac{\|\psi_1(X_1)\|^2 z_1 \hat{\theta}_1}{2a_1^2} \right) + \frac{5}{4} + b_{\max}^2 + y_2^2 + z_2^2 + \sigma_1 \tilde{\theta}_1 \hat{\theta}_1 + \gamma_1 \tilde{b}_m \hat{b}_m \\ & + \gamma_2 \tilde{\Theta} \hat{\Theta} - |z_1|^{2q} + \frac{a_1^2}{2} - 3z_1^2, \end{aligned} \quad (3.47)$$

where there exists a non-negative continuous function $S(z_1, \hat{\Theta}, \hat{b}_m, \hat{\theta}_1, \Upsilon, \Xi, \bar{\lambda}_{m+2}, y_d, r, \bar{\lambda}_2)$, such that:

$$\begin{aligned} & \left| \delta_1 - \frac{\beta}{\hat{b}_m^2 + \beta} \left(-(k_1 + 3) z_1 - \Upsilon_2 - \varpi^T \hat{\Theta} - \frac{\|\psi_1(X_1)\|^2 z_1 \hat{\theta}_1}{2a_1^2} \right) \right| \\ & \leq S(z_1, \hat{\Theta}, \hat{b}_m, \hat{\theta}_1, \Upsilon, \Xi, \bar{\lambda}_{m+2}, y_d, r, \bar{\lambda}_2). \end{aligned} \quad (3.48)$$

There exists a non-negative continuous function $K_1(z_1, y_d, \dot{y}_d, r, \bar{\lambda}_2)$ such that the absolute value of $B_1(X_1)$ is bounded by $K_1(z_1, y_d, \dot{y}_d, r, \bar{\lambda}_2)$. According to Young's inequality:

$$z_1 \varepsilon_1 \leq z_1^2 + \frac{1}{4} \varepsilon_1^2. \quad (3.49)$$

$$z_1 B_1(X_1) \leq z_1^2 + \frac{1}{4} K_1^2. \quad (3.50)$$

$$z_1 S \leq z_1^2 + \frac{1}{4} S^2. \quad (3.51)$$

Utilizing Eq (3.49) through (3.51), Eq (3.47) can be reformulated as:

$$\begin{aligned} \dot{V}_{z_1} \leq & - \left(k_1 - \frac{b_{\max}^2}{2} \right) z_1^2 + \frac{5}{4} + b_{\max}^2 + y_2^2 + z_2^2 + \sigma_1 \tilde{\theta}_1 \hat{\theta}_1 + \gamma_1 \tilde{b}_m \hat{b}_m \\ & + \gamma_2 \tilde{\Theta} \hat{\Theta} - |z_1|^{2q} + \frac{a_1^2}{2} + \frac{1}{4} \varepsilon_1^2 + \frac{1}{4} K_1^2 + \frac{1}{4} S^2. \end{aligned} \quad (3.52)$$

According to Young's inequality:

$$\begin{aligned} \sigma_1 \tilde{\theta}_1 \hat{\theta}_1 & \leq -\frac{\sigma_1}{2} \tilde{\theta}_1^2 + \frac{\sigma_1}{2} \theta_1^2 \\ & \leq -\sigma_1 \frac{1-q}{2} \tilde{\theta}_1^2 + \frac{\sigma_1}{2} \theta_1^2 - \sigma_1 \frac{q}{2} \tilde{\theta}_1^2. \end{aligned} \quad (3.53)$$

Applying Lemma 4 with $x = \tilde{\theta}_1^{2q}, y = 1, a = \frac{1}{q} > 1$, and $b = \frac{1}{1-q}$, we obtain:

$$\begin{aligned} \tilde{\theta}_1^{2q} & \leq q \left(\tilde{\theta}_1^{2q} \right)^{\frac{1}{q}} + (1-q) \\ & = q \tilde{\theta}_1^2 + (1-q). \end{aligned} \quad (3.54)$$

Therefore

$$-\sigma_1 \frac{q}{2} \tilde{\theta}_1^2 \leq -\frac{\sigma_1 \tilde{\theta}_1^{2q}}{2} + \frac{\sigma_1(1-q)}{2}. \quad (3.55)$$

Substitute Eq (3.55) into Eq (3.53) to obtain:

$$\sigma_1 \tilde{\theta}_1 \hat{\theta}_1 \leq -\sigma_1 \frac{1-q}{2} \tilde{\theta}_1^2 + \frac{\sigma_1}{2} \theta_1^2 - \frac{\sigma_1 \tilde{\theta}_1^{2q}}{2} + \frac{\sigma_1(1-q)}{2}. \quad (3.56)$$

Similarly, it can be proved:

$$\gamma_1 \tilde{b}_m \hat{b}_m \leq -\gamma_1 \frac{1-q}{2} \tilde{b}_m^2 + \frac{\gamma_1}{2} b_m^2 - \frac{\gamma_1 \tilde{b}_m^{2q}}{2} + \frac{\gamma_1(1-q)}{2}. \quad (3.57)$$

$$\gamma_2 \tilde{\Theta} \hat{\Theta} \leq -\gamma_2 \frac{1-q}{2} \tilde{\Theta}^2 + \frac{\gamma_2}{2} \Theta^2 - \frac{\gamma_2 \tilde{\Theta}^{2q}}{2} + \frac{\gamma_2(1-q)}{2}. \quad (3.58)$$

Therefore, Eq (3.52) is rewritten as

$$\begin{aligned} \dot{V}_{z_1} \leq & -\left(k_1 - \frac{b_{\max}^2}{2}\right)z_1^2 + \frac{5}{4} + b_{\max}^2 + y_2^2 + z_2^2 - \sigma_1 \frac{1-q}{2} \tilde{\theta}_1^2 + \frac{\sigma_1}{2} \theta_1^2 \\ & - \frac{\sigma_1 \tilde{\theta}_1^{2q}}{2} + \frac{\sigma_1(1-q)}{2} - \gamma_1 \frac{1-q}{2} \tilde{b}_m^2 + \frac{\gamma_1}{2} b_m^2 - \frac{\gamma_1 \tilde{b}_m^{2q}}{2} + \frac{\gamma_1(1-q)}{2} \\ & - \gamma_2 \frac{1-q}{2} \tilde{\Theta}^2 + \frac{\gamma_2}{2} \Theta^2 - \frac{\gamma_2 \tilde{\Theta}^{2q}}{2} + \frac{\gamma_2(1-q)}{2} - |z_1|^{2q} + \frac{a_1^2}{2} + \frac{1}{4} \varepsilon_1^2 + \frac{1}{4} K_1^2 + \frac{1}{4} S^2. \end{aligned} \quad (3.59)$$

If $V_1 = V_\varepsilon + V_{z_1} + \frac{r}{\lambda_0}$, then:

$$\begin{aligned} \dot{V}_1 &= \dot{V}_\varepsilon + \dot{V}_{z_1} + \frac{\dot{r}}{\lambda_0} \\ &\leq -(h-2)\varepsilon^T \varepsilon + \sum_{j=1}^n \|p\|^2 \|\delta_j\|^2 + 2 \sum_{j=1}^n \|p\|^2 \Delta_{j_1}^2(|y|) + \|p\|^2 \varphi_0(r) + \|p\|^2 \vartheta_0^* \\ &\quad - \left(k_1 - \frac{b_{\max}^2}{2}\right)z_1^2 + \frac{5}{4} + b_{\max}^2 + y_2^2 + z_2^2 - \sigma_1 \frac{1-q}{2} \tilde{\theta}_1^2 + \frac{\sigma_1}{2} \theta_1^2 - \frac{\sigma_1 \tilde{\theta}_1^{2q}}{2} + \frac{\sigma_1(1-q)}{2} \\ &\quad - \gamma_1 \frac{1-q}{2} \tilde{b}_m^2 + \frac{\gamma_1}{2} b_m^2 - \frac{\gamma_1 \tilde{b}_m^{2q}}{2} + \frac{\gamma_1(1-q)}{2} - \gamma_2 \frac{1-q}{2} \tilde{\Theta}^2 + \frac{\gamma_2}{2} \Theta^2 \\ &\quad - \frac{\gamma_2 \tilde{\Theta}^{2q}}{2} + \frac{\gamma_2(1-q)}{2} - |z_1|^{2q} + \frac{a_1^2}{2} + \frac{1}{4} \varepsilon_1^2 + \frac{1}{4} K_1^2 + \frac{1}{4} S^2 - \frac{\bar{c}r}{\lambda_0} + \frac{\bar{\Lambda}(|y|)}{\lambda_0} + \frac{d}{\lambda_0} \\ &\leq -\left(h - \frac{9}{4}\right)\varepsilon^T \varepsilon + \|p\|^2 \vartheta_0^* - k_1 z_1^2 - |z_1|^{2q} - \sigma_1 \frac{1-q}{2} \tilde{\theta}_1^2 - \frac{\sigma_1 \tilde{\theta}_1^{2q}}{2} + y_2^2 + z_2^2 \\ &\quad - \gamma_1 \frac{1-q}{2} \tilde{b}_m^2 - \frac{\gamma_1 \tilde{b}_m^{2q}}{2} - \gamma_2 \frac{1-q}{2} \tilde{\Theta}^2 - \frac{\gamma_2 \tilde{\Theta}^{2q}}{2} + \frac{1}{4} K_1^2 + \frac{1}{4} S^2 - \frac{\bar{c}r}{\lambda_0} + Q(y, r) \\ &\quad + \frac{5}{4} + b_{\max}^2 + \frac{\sigma_1}{2} \theta_1^2 + \frac{\sigma_1(1-q)}{2} + \frac{\gamma_1}{2} b_m^2 + \frac{\gamma_1(1-q)}{2} + \frac{\gamma_2}{2} \Theta^2 + \frac{\gamma_2(1-q)}{2} + \frac{a_1^2}{2} + \frac{d}{\lambda_0}, \end{aligned} \quad (3.60)$$

where

$$Q(y, r) = \sum_{j=1}^n \|p\|^2 \|\delta_j\|^2 + 2 \sum_{j=1}^n \|p\|^2 \Delta_{j_1}^2(|y|) + \|p\|^2 \varphi_0(r) + \frac{\bar{\Lambda}(|y|)}{\lambda_0}.$$

Using Lemma 4, we derive the following:

$$\begin{aligned} -\left(h - \frac{9}{4}\right)\varepsilon^T \varepsilon &\leq -\frac{h - \frac{9}{4}}{2\lambda_{\max}(p)} \varepsilon^T p \varepsilon - \frac{h - \frac{9}{4}}{2\lambda_{\max}(p)} \varepsilon^T p \varepsilon \\ &\leq -\frac{h - \frac{9}{4}}{2\lambda_{\max}(p)q} (\varepsilon^T p \varepsilon)^q + \frac{\left(h - \frac{9}{4}\right)(1-q)}{2\lambda_{\max}(p)q} - \frac{h - \frac{9}{4}}{2\lambda_{\max}(p)} \varepsilon^T p \varepsilon \end{aligned} \quad (3.61)$$

$$\begin{aligned} -\frac{\bar{c}r}{\lambda_0} &\leq -\frac{\bar{c}r}{2\lambda_0} - \frac{\bar{c}r}{2\lambda_0} \\ &\leq -\frac{\bar{c}}{2\lambda_0 q} r^q + \frac{\bar{c}(1-q)}{2\lambda_0 q} - \frac{\bar{c}r}{2\lambda_0}. \end{aligned} \quad (3.62)$$

Then, Eq (3.60) can be transformed into

$$\begin{aligned} \dot{V}_1 \leq & -\frac{h - \frac{9}{4}}{2\lambda_{\max}(p)q} (\varepsilon^T p \varepsilon)^q - \frac{h - \frac{9}{4}}{2\lambda_{\max}(p)} \varepsilon^T p \varepsilon - \left(k_1 - \frac{b_{\max}^2}{2}\right) z_1^2 - |z_1|^{2q} \\ & - \sigma_1 \frac{1-q}{2} \tilde{\theta}_1^2 - \frac{\sigma_1 \tilde{\theta}_1^{2q}}{2} + y_2^2 + z_2^2 - \gamma_1 \frac{1-q}{2} \tilde{b}_m^2 - \frac{\gamma_1 \tilde{b}_m^{2q}}{2} - \gamma_2 \frac{1-q}{2} \tilde{\Theta}^2. \\ & - \frac{\gamma_2 \tilde{\Theta}^{2q}}{2} + \frac{1}{4} K_1^2 + \frac{1}{4} S^2 - \frac{\bar{c}}{2\lambda_0 q} r^q - \frac{\bar{c}r}{2\lambda_0} + Q(y, r) + C_1, \end{aligned} \quad (3.63)$$

where

$$\begin{aligned} C_1 = & \frac{5}{4} + b_{\max}^2 + \frac{\sigma_1}{2} \theta_1^2 + \frac{\sigma_1(1-q)}{2} + \frac{\gamma_1}{2} b_m^2 + \frac{\gamma_1(1-q)}{2} + \frac{\gamma_2}{2} \Theta^2 + \frac{\gamma_2(1-q)}{2} \\ & + \frac{a_1^2}{2} + \frac{d}{\lambda_0} + \frac{\left(h - \frac{9}{4}\right)(1-q)}{2\lambda_{\max}(p)q} + \frac{\bar{c}(1-q)}{2\lambda_0 q} + \|p\|^2 \vartheta_0^*. \end{aligned}$$

For $i = 2$, the first-order filter is designed as follows:

$$\begin{aligned} \tau_i \dot{\omega}_i &= \text{sig}(\alpha_{i-1} - \omega_i)^{2q-1} + \text{sig}(\alpha_{i-1} - \omega_i) - \dot{\omega}_i \\ &= \frac{1}{\tau_i} |y_i|^{2q-1} \text{sgn}(y_i) + \frac{1}{\tau_i} |y_i| \text{sgn}(y_i) \\ &\leq \frac{1}{\tau_i^2} |y_i|^{4p-2} + \frac{1}{\tau_i^2} y_i^2 + \frac{1}{2}, \end{aligned} \quad (3.64)$$

where $\tau_i > 0$ is a design constant.

Step i (where $2 \leq i \leq s-1$), define the i th dynamic layer as:

$$z_i = v_{m,i} - \omega_i - \tilde{\lambda}_i. \quad (3.65)$$

The time derivative of the dynamic layer z_i is expressed as:

$$\begin{aligned} \dot{z}_i &= \dot{v}_{m,i} - \dot{\omega}_i - \dot{\omega}_i - \dot{\tilde{\lambda}}_i \\ &= z_{i+1} + y_{i+1} + \alpha_i - l_i v_{m,1} - \dot{\omega}_i + c_i \omega_i - \tilde{\lambda}_i. \end{aligned} \quad (3.66)$$

A Lyapunov function is selected as

$$V_i = V_{i-1} + \frac{1}{2} z_i^2 + \frac{1}{2} \tilde{\theta}_i^2 + \frac{1}{2} y_i^2. \quad (3.67)$$

Take the derivative of V_i about t and get:

$$\begin{aligned} \dot{V}_i &= \dot{V}_{i-1} + z_i \dot{z}_i - \tilde{\theta}_i \dot{\tilde{\theta}}_i + y_i \dot{y}_i \\ &= \dot{V}_{i-1} + z_i (z_{i+1} + y_{i+1} + \alpha_i - l_i v_{m,1} - \dot{\omega}_i + c_i \omega_i - \tilde{\lambda}_i) - \tilde{\theta}_i \dot{\tilde{\theta}}_i + y_i \dot{y}_i. \end{aligned} \quad (3.68)$$

Based on Eqs (3.70) and (3.71), we can further simplify Eq (3.69):

$$\dot{V}_i \leq \dot{V}_{i-1} + z_i \left(z_{i+1} + y_{i+1} + \alpha_i - l_i v_{m,1} + \frac{1}{\tau_i^2} |y_i|^{4p-2} + \frac{1}{\tau_i^2} y_i^2 + \frac{1}{2} + c_i \tilde{\lambda}_i \right) - \tilde{\theta}_i \dot{\tilde{\theta}}_i + y_i \dot{y}_i. \quad (3.69)$$

Applying Young's inequality, we find:

$$z_i z_{i+1} \leq \frac{1}{4} z_i^2 + z_{i+1}^2, \quad (3.70)$$

$$z_i y_{i+1} \leq \frac{1}{4} z_i^2 + y_{i+1}^2. \quad (3.71)$$

Using Lemma 5 Young's inequality, Eq (3.69) can be transformed as follows:

$$\begin{aligned} \dot{V}_i &\leq \dot{V}_{i-1} + z_i \left(z_{i+1} + y_{i+1} + \alpha_i - l_i v_{m,1} + \frac{1}{\tau_i^2} |y_i|^{4p-2} + \frac{1}{\tau_i^2} y_i^2 + \frac{1}{2} + c_i \lambda_i \right) - \tilde{\theta}_i \dot{\hat{\theta}}_i + y_i \dot{y}_i \\ &\leq \dot{V}_{i-1} + z_i \left(\frac{1}{2} z_i + \alpha_i - l_i v_{m,1} + \frac{1}{\tau_i^2} |y_i|^{4p-2} + \frac{1}{\tau_i^2} y_i^2 + \frac{1}{2} + c_i \lambda_i \right) \\ &\quad - \tilde{\theta}_i \dot{\hat{\theta}}_i + y_i \dot{y}_i + z_{i+1}^2 + y_{i+1}^2. \end{aligned} \quad (3.72)$$

Let

$$H_i(X_i) = \frac{1}{\tau_i^2} |y_i|^{4p-2} + \frac{1}{\tau_i^2} y_i^2 + \frac{1}{2} + c_i \lambda_i + |z_i|^{2q-1},$$

where $X_i = [z_i, y_i, \lambda_i]^T$, then

$$\begin{aligned} \dot{V}_i &\leq \dot{V}_{i-1} + z_i \left(\frac{1}{2} z_i + \alpha_i - l_i v_{m,1} + W_{hi}^{*T} \psi_i(X_i) + B_i(X_i) \right) \\ &\quad - \tilde{\theta}_i \dot{\hat{\theta}}_i + y_i \dot{y}_i + z_{i+1}^2 + y_{i+1}^2 - |z_i|^{2q}. \end{aligned} \quad (3.73)$$

Using Young's inequality as shown in Eq (3.74), we can transform Eq (3.73) into:

$$z_i W_{hi}^{*T} \psi_i(X_i) \leq \frac{\|\psi_i(X_i)\|^2 z_i^2 \theta_i}{2a_i^2} + \frac{a_i^2}{2}, \quad (3.74)$$

where $a_i > 0$ serves as a design constant that helps balance the trade-off between the growth of the Lyapunov function due to the nonlinearity in the system and the control effort.

$$\begin{aligned} \dot{V}_i &\leq \dot{V}_{i-1} + z_i \left(\frac{1}{2} z_i + \alpha_i - l_i v_{m,1} + \frac{\|\psi_i(X_i)\|^2 z_i \theta_i}{2a_i^2} + B_i(X_i) \right) \\ &\quad - \tilde{\theta}_i \dot{\hat{\theta}}_i + y_i \dot{y}_i + z_{i+1}^2 + y_{i+1}^2 - |z_i|^{2q} + \frac{a_i^2}{2}. \end{aligned} \quad (3.75)$$

The virtual control law is designed as follows:

$$\alpha_i = - \left(k_i + \frac{5}{2} \right) z_i + l_i v_{m,1} \frac{\|\psi_i(X_i)\|^2 z_i \hat{\theta}_i}{2a_i^2}. \quad (3.76)$$

The adaptive law is designed as follows:

$$\dot{\hat{\theta}}_i = \frac{\|\psi_i(X_i)\|^2 z_i^2}{2a_i^2} - \sigma_i \hat{\theta}_i, \quad (3.77)$$

where $k_i > 0, \sigma_i > 0$ is the design constant.

Substituting the Eqs (3.76) and (3.77) into the Eq (3.75), we get

$$\begin{aligned} \dot{V}_i &\leq \dot{V}_{i-1} + z_i B_i(X_i) + \sigma_i \tilde{\theta}_i \hat{\theta}_i + y_i \dot{y}_i + z_{i+1}^2 + y_{i+1}^2 - |z_i|^{2q} + \frac{a_i^2}{2} - 2z_i^2 \\ &\leq \dot{V}_{i-1} + z_i B_i(X_i) + y_i \dot{y}_i + z_{i+1}^2 + y_{i+1}^2 - |z_i|^{2q} + \frac{a_i^2}{2} - 2z_i^2 \\ &\quad - \sigma_i \frac{1-q}{2} \tilde{\theta}_i^2 + \frac{\sigma_i}{2} \theta_i^2 - \frac{\sigma_i \tilde{\theta}_i^{2q}}{2} + \frac{\sigma_i(1-q)}{2}. \end{aligned} \quad (3.78)$$

There is a nonnegative continuous function $K_i(z_i, y_i, \lambda_i)$, which makes $|B_i(X_i)| \leq K_i(z_i, y_i, \lambda_i)$.

From Young's:

$$z_i B_i(X_i) \leq z_i^2 + \frac{1}{4} K_i^2. \quad (3.79)$$

Based on Eqs (3.79) and (3.78) can be reformulated as:

$$\begin{aligned} \dot{V}_i &\leq \dot{V}_{i-1} + y_i \dot{y}_i + z_{i+1}^2 + y_{i+1}^2 - |z_i|^{2q} + \frac{a_i^2}{2} - z_i^2 - k_i z_i^2 \\ &\quad - \sigma_i \frac{1-q}{2} \tilde{\theta}_i^2 + \frac{\sigma_i}{2} \theta_i^2 - \frac{\sigma_i \tilde{\theta}_i^{2q}}{2} + \frac{\sigma_i(1-q)}{2} + \frac{1}{4} K_i^2 \\ &\leq -\frac{h-\frac{9}{4}}{2\lambda_{\max}(p)q} (\varepsilon^T p \varepsilon)^q - \frac{h-\frac{9}{4}}{2\lambda_{\max}(p)} \varepsilon^T p \varepsilon + \frac{1}{4} S^2 - \frac{\bar{c}}{2\lambda_0 q} r^q - \frac{\bar{c}r}{2\lambda_0} \\ &\quad + Q(y, r) - \gamma_1 \frac{1-q}{2} \tilde{b}_m^2 - \frac{\gamma_1 \tilde{b}_m^{2q}}{2} - \gamma_2 \frac{1-q}{2} \tilde{\Theta}^2 - \frac{\gamma_2 \tilde{\Theta}^{2q}}{2} - \sum_{j=2}^i k_j z_j^2 \\ &\quad - \left(k_1 - \frac{b_{\max}^2}{2}\right) z_1^2 - \sum_{j=1}^i |z_j|^{2q} - \sum_{j=1}^i \sigma_j \frac{1-q}{2} \tilde{\theta}_j^2 - \sum_{j=1}^i \frac{\sigma_j \tilde{\theta}_j^{2q}}{2} + \sum_{j=1}^i \left(\frac{1}{4} K_j^2 + C_j\right) \\ &\quad + \sum_{j=1}^{i-1} \left[-\frac{1}{\tau_j} |y_j|^{2q} - \left(\frac{1}{\tau_j} - 2\right) y_j^2 + \frac{1}{4} \eta_j^2\right] + y_i \dot{y}_i + z_{i+1}^2 + y_{i+1}^2 + y_i^2, \end{aligned} \quad (3.80)$$

where

$$C_i = \frac{a_i^2}{2} + \frac{\sigma_i}{2} \theta_i^2 + \frac{\sigma_i(1-q)}{2}.$$

The first-order nonlinear filter is introduced as follows:

$$\dot{\omega}_i = -\frac{1}{\tau_i} \text{sig}(y_i)^{2q-1} - \frac{1}{\tau_i} \text{sig}(y_i), \quad (3.81)$$

where τ_i is a positive design constant, α_{i-1} and ω_i are the input and output of the first-order filter, respectively.

Assuming the existence of a non-negative continuous function $\eta_i(\bar{z}_i, \bar{y}_i, \bar{\theta}_i, \hat{b}_m, \hat{\Theta}, y_d, \dot{y}_d, \ddot{y}_d, r, \bar{\pi}_i)$, it can be stated that:

$$|-\dot{\alpha}_{i-1}| \leq \eta_i(\bar{z}_i, \bar{y}_i, \bar{\theta}_i, \hat{b}_m, \hat{\Theta}, y_d, \dot{y}_d, \ddot{y}_d, r, \bar{\lambda}_i), \quad (3.82)$$

$$\begin{aligned}
y_i \dot{y}_i &= y_i (\dot{\omega}_i - \dot{\alpha}_{i-1}) \\
&= -\frac{1}{\tau_i} |y_i|^{2q} - \frac{1}{\tau_i} y_i^2 - y_i \dot{\alpha}_{i-1} \\
&\leq -\frac{1}{\tau_i} |y_i|^{2q} - \frac{1}{\tau_i} y_i^2 + y_i^2 + \frac{1}{4} \eta_i^2.
\end{aligned} \tag{3.83}$$

Substituting the Eq (3.83) into the Eq (3.80)

$$\begin{aligned}
\dot{V}_i &\leq -\frac{h - \frac{9}{4}}{2\lambda_{\max}(p)q} (\varepsilon^T p \varepsilon)^q - \frac{h - \frac{9}{4}}{2\lambda_{\max}(p)} \varepsilon^T p \varepsilon + \frac{1}{4} S^2 - \frac{\bar{c}}{2\lambda_0 q} r^q - \frac{\bar{c}r}{2\lambda_0} \\
&\quad + Q(y, r) - \gamma_1 \frac{1-q}{2} \tilde{b}_m^2 - \frac{\gamma_1 \tilde{b}_m^{2q}}{2} - \gamma_2 \frac{1-q}{2} \tilde{\Theta}^2 - \frac{\gamma_2 \tilde{\Theta}^{2q}}{2} - \sum_{j=2}^i k_j z_j^2 \\
&\quad - \left(k_1 - \frac{b_{\max}^2}{2} \right) z_1^2 - \sum_{j=1}^i |z_j|^{2q} - \sum_{j=1}^i \sigma_j \frac{1-q}{2} \tilde{\theta}_j^2 - \sum_{j=1}^i \frac{\sigma_j \tilde{\theta}_j^{2q}}{2} + \sum_{j=1}^i \left(\frac{1}{4} K_j^2 + C_j \right) \\
&\quad + \sum_{j=1}^i \left[-\frac{1}{\tau_j} |y_j|^{2q} - \left(\frac{1}{\tau_j} - 2 \right) y_j^2 + \frac{1}{4} \eta_j^2 \right] + z_{i+1}^2 + y_{i+1}^2.
\end{aligned} \tag{3.84}$$

Here is a reformulated expression of your description of a first-order filter:

$$\begin{aligned}
\tau_s \dot{\omega}_s &= \text{sig}(\alpha_{s-1} - \omega_s)^{2q-1} + \text{sig}(\alpha_{s-1} - \omega_s) \\
&= \frac{1}{\tau_s} |y_s|^{2q-1} \text{sgn}(y_s) + \frac{1}{\tau_s} |y_s| \text{sgn}(y_s) - \dot{\omega}_s \\
&\leq \frac{1}{\tau_s^2} |y_s|^{4p-2} + \frac{1}{\tau_s^2} y_s^2 + \frac{1}{2},
\end{aligned} \tag{3.85}$$

where ω_s is the output of the first-order filter with α_{s-1} as input, and $\tau_s > 0$ is a design constant.

Step ρ : Define the ρ th dynamic surface

$$z_\rho = v_{m,\rho} - \omega_\rho - \lambda_\rho. \tag{3.86}$$

The derivative of z_ρ with respect to time t is

$$\begin{aligned}
\dot{z}_\rho &= \dot{v}_{m,\rho} - \dot{\omega}_\rho - \dot{\lambda}_\rho \\
&= v_{m,\rho+1} - l_\rho v_{m,1} - \dot{\omega}_\rho + c_\rho \lambda_\rho + q(v).
\end{aligned} \tag{3.87}$$

Select a Lyapunov function as:

$$V_\rho = V_{\rho-1} + \frac{1}{2} z_\rho^2 + \frac{1}{2} \tilde{\theta}_\rho^2 + \frac{1}{2} y_\rho^2. \tag{3.88}$$

The design control law is as follows:

$$v = -(k_\rho + 3) z_\rho - v_{m,\rho+1} + l_\rho v_{m,1} - \frac{\|\psi_\rho(X_\rho)\|^2 z_\rho \hat{\theta}_\rho}{2\alpha_\rho^2}. \tag{3.89}$$

An adaptive law is designed as follows:

$$\dot{\hat{\theta}}_\rho = \frac{\|\psi_\rho(X_\rho)\|^2 z_\rho^2}{2a_\rho^2} - \sigma_\rho \hat{\theta}_\rho, \quad (3.90)$$

where $k_\rho > 0$, and $\sigma_\rho > 0$ are design constants.

The proof process of ρ step is similar to the previous one, so I won't repeat it here. Therefore, the derivative of V_ρ is

$$\begin{aligned} \dot{V}_\rho \leq & -\frac{h - \frac{\rho}{4}}{2\lambda_{\max}(p)q} (\varepsilon^T p \varepsilon)^q - \frac{h - \frac{\rho}{4}}{2\lambda_{\max}(p)} \varepsilon^T p \varepsilon + \frac{1}{4} S^2 - \frac{\bar{c}}{2\lambda_0 q} r^q - \frac{\bar{c}r}{2\lambda_0} \\ & + Q(y, r) - \gamma_1 \frac{1-q}{2} \tilde{b}_m^2 - \frac{\gamma_1 \tilde{b}_m^{2q}}{2} - \gamma_2 \frac{1-q}{2} \tilde{\Theta}^2 - \frac{\gamma_2 \tilde{\Theta}^{2q}}{2} - \sum_{j=2}^{\rho} k_j z_j^2 \\ & - \left(k_1 - \frac{b_{\max}^2}{2}\right) z_1^2 - \sum_{j=1}^{\rho} |z_j|^{2q} - \sum_{j=1}^{\rho} \sigma_j \frac{1-q}{2} \tilde{\theta}_j^2 - \sum_{j=1}^{\rho} \frac{\sigma_j \tilde{\theta}_j^{2q}}{2} + \sum_{j=1}^{\rho} \left(\frac{1}{4} K_j^2 + C_j\right) \\ & + \sum_{j=2}^{\rho} \left[-\frac{1}{\tau_j} |y_j|^{2q} - \left(\frac{1}{\tau_j} - 2\right) y_j^2 + \frac{1}{4} \eta_j^2\right]. \end{aligned} \quad (3.91)$$

3.4. Stability analysis

The compact set Ω is specified by the vector components:

$$\Omega = \left\{ \left[\bar{z}_\rho, \bar{y}_\rho, \bar{\theta}_\rho, \bar{b}_m, \bar{\Theta}, r, \varepsilon \right]^T : V = V_\rho \leq P \right\}, \quad (3.92)$$

where P represents any positive constant. On the compact set $\Omega \times \Omega_d$, the non-negative continuous function $\eta_i(\cdot)$ attains a maximum value of M_i . The non-negative continuous function $K_i(\cdot)$ reaches a maximum value of N_i on the same set, and the non-negative continuous function S achieves a maximum value of N_0 on this set.

Theorem 1. Consider a closed-loop system composed of system Eq (2.1), control law Eq (3.89), virtual control laws Eqs (3.76) and (3.43), along with adaptive laws Eqs (3.44)–(3.46), Eqs (3.77) and (3.90). If Assumptions 1–4 hold, and the initial condition satisfies $V(0) \leq P$, by appropriately choosing positive constants $k_i, \tau_i, \sigma_i, \gamma_1, \gamma_2, h, \bar{c}$, the boundedness of all signals within the closed-loop system can be ensured. Furthermore, the design constants $k_i, \tau_i, \sigma_i, \gamma_1, \gamma_2, h, \bar{c}$, the boundedness of all signals within the system can be ensured, achieving practically finite-time stability.

$$\begin{cases} k_1 \geq \frac{b_{\max}^2}{2} + \frac{\alpha_0}{2}, h > \frac{\rho}{4}, \sigma_i > 0, \gamma_1 > 0, \bar{c} > 0, \gamma_2 > 0, i = 1, \dots, \rho \\ k_j \geq \frac{\alpha_0}{2}, \frac{1}{\tau_j} \geq 2, j = 2, \dots, \rho \\ \alpha_0 \leq \min \left\{ \sigma_i (1-q), \frac{h - \frac{\rho}{4}}{2\lambda_{\max}(p)}, \gamma_1 (1-q), \gamma_2 (1-q), \frac{\bar{c}}{2}, \frac{1}{\tau_j} - 2 \right\} \\ \beta_0 \leq \min \left\{ 2^q, 2^{q-1} \sigma_i, \frac{h - \frac{\rho}{4}}{2\lambda_{\max}(p)q}, \gamma_1 2^{q-1}, \gamma_2 2^{1-q}, \frac{\bar{c} \lambda_0^{q-1}}{2q}, \frac{1}{\tau_j} 2^q \right\} \end{cases}. \quad (3.93)$$

The Lyapunov function is defined as follows:

$$V = V_\rho = V_\varepsilon + \frac{r}{\lambda_0} + \sum_{i=1}^{\rho} \frac{1}{2} z_i^2 + \sum_{i=1}^{\rho} \frac{1}{2} \tilde{\theta}_i^2 + \sum_{i=1}^{\rho} \frac{1}{2} y_i^2 + \frac{1}{2} \tilde{b}_m^2 + \frac{1}{2} \tilde{\Theta}^2. \quad (3.94)$$

The time derivative of V is

$$\begin{aligned}
\dot{V} &\leq -\frac{h - \frac{9}{4}}{2\mathfrak{L}_{\max}(p)q} (\varepsilon^T p \varepsilon)^q - \frac{h - \frac{9}{4}}{2\mathfrak{L}_{\max}(p)} \varepsilon^T p \varepsilon - \frac{\bar{c}}{2\mathfrak{L}_0 q} r^q - \frac{\bar{c}r}{2\mathfrak{L}_0} \\
&+ Q(y, r) - \gamma_1 \frac{1-q}{2} \tilde{b}_m^2 - \frac{\gamma_1 \tilde{b}_m^{2q}}{2} - \gamma_2 \frac{1-q}{2} \tilde{\Theta}^2 - \frac{\gamma_2 \tilde{\Theta}^{2q}}{2} - \sum_{i=2}^{\rho} k_i z_i^2 \\
&- \left(k_1 - \frac{b_{\max}^2}{2} \right) z_1^2 - \sum_{i=1}^{\rho} |z_i|^{2q} - \sum_{i=1}^{\rho} \sigma_i \frac{1-q}{2} \tilde{\theta}_i^2 - \sum_{i=1}^{\rho} \frac{\sigma_i \tilde{\theta}_i^{2q}}{2} + \sum_{i=1}^{\rho} \left(\frac{1}{4} N_i^2 + C_i \right) \\
&+ \sum_{i=2}^{\rho} \left[-\frac{1}{\tau_i} |y_i|^{2q} - \left(\frac{1}{\tau_i} - 2 \right) y_i^2 + \frac{1}{4} M_i^2 \right] + \frac{1}{4} N_0^2 \tag{3.95} \\
&\leq \left[-\sum_{i=2}^{\rho} k_i z_i^2 - \left(k_1 - \frac{b_{\max}^2}{2} \right) z_1^2 - \frac{h - \frac{9}{4}}{2\mathfrak{L}_{\max}(p)} \varepsilon^T p \varepsilon - \frac{\bar{c}r}{2\mathfrak{L}_0} - \gamma_1 \frac{1-q}{2} \tilde{b}_m^2 \right. \\
&- \gamma_2 \frac{1-q}{2} \tilde{\Theta}^2 - \sum_{i=1}^{\rho} \sigma_i \frac{1-q}{2} \tilde{\theta}_i^2 - \sum_{i=2}^{\rho} \left(\frac{1}{\tau_i} - 2 \right) y_i^2 \left. \right] + \left[-\frac{h - \frac{9}{4}}{2\mathfrak{L}_{\max}(p)q} (\varepsilon^T p \varepsilon)^q \right. \\
&- \frac{\bar{c}}{2\mathfrak{L}_0 q} r^q - \frac{\gamma_1 \tilde{b}_m^{2q}}{2} - \frac{\gamma_2 \tilde{\Theta}^{2q}}{2} - \sum_{i=1}^{\rho} |z_i|^{2q} - \sum_{i=1}^{\rho} \frac{\sigma_i \tilde{\theta}_i^{2q}}{2} - \sum_{i=2}^{\rho} \frac{1}{\tau_i} |y_i|^{2q} \left. \right] + C + Q(y, r),
\end{aligned}$$

where

$$C = \sum_{i=1}^{\rho} \left(\frac{1}{4} N_i^2 + C_i \right) + \sum_{i=2}^{\rho} \frac{1}{4} M_i^2 + \frac{1}{4} N_0^2. \tag{3.96}$$

If $V(t) \leq P$, then the variables $\bar{z}_\rho, \bar{y}_\rho, \hat{\theta}_\rho, \hat{b}_m, \hat{\Theta}, r, \varepsilon, y$ are all bounded. From the equation $z_1 = y - y_d - \lambda_1$, it is evident that λ_1 is bounded. Furthermore, according to Eq (3.26), λ_i is confirmed to be bounded. Based on Eq (3.17), it is known that ζ and Ξ are bounded as well. From system Eq (2.1) and the third expression in Eq (3.17), it can be seen that

$$\lambda_i = \frac{s^{i-1} + l_1 s^{i-2} + \dots + l_{i-1}}{L(s)B(s)} \left\{ \frac{d^n y}{dt^n} - \sum_{i=1}^n \frac{d^{n-1} y}{dt^{n-1}} [f_i(y) + d_i(\xi, y, t)] \right\}. \tag{3.97}$$

Given that $L(s) = |sI - A_0| = s^n + l_1 s^{n-1} + \dots + l_{n-1} s + l_n$, and considering that $f_i(y)$ and $d_i(\xi, y, t)$ are smooth functions, it follows that the values $\lambda_1, \dots, \lambda_{m+1}$ are bounded. In conjunction with Eq (3.13), this ensures that the variables $v_{m,1}, v_{m-1,2}, \dots, v_{0,2}$ are also bounded. From Eq (3.43), we can see that α_1 is bounded. With $v_{m,2} = z_2 + y_2 + \alpha_1 + \lambda_1$, it is clear that $v_{m,2}$ is bounded. Referring to Eq (3.89), we find that the control law is also bounded. Consequently, Eq (3.95) can be simplified as follows:

$$\dot{V} \leq -\alpha_0 V - \beta_0 V^q + C + Q(y, r). \tag{3.98}$$

Given that $Q(y, r)$ is a non-negative continuous function and the variables y and r are bounded, it follows that $Q(y, r)$ is likewise bounded. Consequently, there is an unknown positive constant μ_0 such that $Q(y, r) \leq \mu_0$. Hence, Eq (3.98) can be simplified as follows:

Where

$$\bar{C} = C + \mu_0.$$

If $V = P$ and $\alpha_0 > \frac{\bar{C}}{P}$, then $\dot{V}_n \leq 0$. If at the initial time $V(0) \leq P$, then for any $t > 0$, $V(t) \leq P$. Multiply both sides of Eq (3.98) by $e^{\alpha_0 t}$ and then integrate over the interval $[0, t]$:

$$0 \leq V(t) \leq \frac{\bar{C}}{\alpha_0} + \left[V(0) - \frac{\bar{C}}{\alpha_0} \right] e^{-\alpha_0 t}. \quad (3.99)$$

According to Eqs (3.94) and (3.99), and Lemma 2, the settling time T_0 can be estimated as less than or equal to $\frac{1}{\alpha_0(1-q)} \ln \frac{\alpha_0 V^{1-q}(x_0) + v\beta_0}{\alpha_0 (\bar{C}/((1-q)\beta_0))^{(1-q)/q} + v\beta_0}$. This formula provides an upper bound on the time required for the system's state to reach a predefined neighborhood of the equilibrium under the specified conditions.

$$|z_1| \leq \sqrt{\frac{2\bar{C}}{\alpha_0} + 2 \left[V(0) - \frac{\bar{C}}{\alpha_0} \right] e^{-\alpha_0 t}}. \quad (3.100)$$

4. Numerical examples

To assess the efficacy of the control strategy introduced in this research, we explore a particular scenario: An output feedback nonlinear system characterized by unmodeled dynamics and quantized input delays. Through detailed analysis of this system, we aim to comprehensively evaluate the performance of the proposed control approach in real-world settings.

$$\begin{cases} \dot{\zeta} = -2\zeta + y \sin t + 0.5 \\ \dot{x}_1 = x_2 + x_1 e^{-0.5x_1} + 0.5x_1 \zeta \sin(x_1 t) \\ \dot{x}_2 = x_1 x_2^2 + (3 - \cos(x_1 x_2)) q(v(t - \tau)) + 0.1 \zeta^2 \cos(0.5x_2 t) \\ y = x_1 \end{cases} \quad (4.1)$$

Select the desired signal as

$$y_d = 0.5 \sin(t) + 0.5 \sin(0.5t). \quad (4.2)$$

The design of k filter is as follows

$$\begin{cases} \dot{\Upsilon}_1 = -l_1 \Upsilon_1 + \Upsilon_2 + l_1 y \\ \dot{\Upsilon}_2 = -l_2 \Upsilon_1 + l_2 y \\ \dot{\Xi}_1 = \begin{bmatrix} -l_1 & 1 \end{bmatrix} \Xi + \begin{bmatrix} \phi_1^T(y) & 0_{1 \times M_1} \end{bmatrix} \\ \dot{\Xi}_2 = \begin{bmatrix} -l_2 & 0 \end{bmatrix} \Xi + \begin{bmatrix} 0_{1 \times M_2} & \phi_1^T(y) \end{bmatrix} \\ \dot{\lambda}_1 = -l_1 \lambda_1 + \lambda_2 \\ \dot{\lambda}_2 = -l_2 \lambda_1 + q(v(t - \tau)) \end{cases} \quad (4.3)$$

The auxiliary system is described as follows:

$$\begin{cases} \dot{\lambda}_1 = \lambda_2 - c_1 \lambda_1 \\ \dot{\lambda}_2 = -c_2 \lambda_2 + q(v(t - \tau)) - q(v) \end{cases} \quad (4.4)$$

The coordinate change design is as follows:

$$\begin{cases} z_1 = y - y_d - \lambda_1 \\ z_2 = v_{m,2} - \omega_2 - \hat{\lambda}_2 \end{cases} \quad (4.5)$$

A virtual control law α_1 is designed as follows:

$$\alpha_1 = -\frac{\hat{b}_m}{\hat{b}_m^2 + \beta} \left((k_1 + 3) z_1 + \Upsilon_2 + \varpi^T \hat{\Theta} + \frac{\|\psi_1(X_1)\|^2 z_1 \hat{\theta}_1}{2a_1^2} \right). \quad (4.6)$$

The control law v is designed as follows:

$$v = -(k_2 + 3) z_2 - v_{0,2} + l_2 v_{0,1} - \frac{\|\psi_2(X_2)\|^2 z_2 \hat{\theta}_2}{2a_2^2}. \quad (4.7)$$

The adaptive law of design parameters is as follows:

$$\dot{\hat{\theta}}_1 = \frac{\|\psi_1(X_1)\|^2 z_1^2}{2a_1^2} - \sigma_1 \hat{\theta}_1. \quad (4.8)$$

$$\dot{\hat{b}}_m = z_1 \alpha_1 - \gamma_1 \hat{b}_m. \quad (4.9)$$

$$\dot{\hat{\Theta}} = \varpi z_1 - \gamma_2 \hat{\Theta}. \quad (4.10)$$

$$\dot{\hat{\theta}}_2 = \frac{\|\psi_2(X_2)\|^2 z_2^2}{2a_2^2} - \sigma_2 \hat{\theta}_2. \quad (4.11)$$

In this study, we examine two dynamic systems $X_1 = [z_1, y_d, \dot{y}_d, \lambda_1, \lambda_2, r]^T$ and $X_2 = [z_2, y_2, \lambda_2]^T$. The dynamic signal of the system is given by the following equation:

$$\dot{r} = -r + 1.5x_1^4 + 0.8. \quad (4.12)$$

For the simulation and analysis of the system, we set a series of initial conditions and parameter values. The initial state is set to: $x_1(0) = 0.1, x_2(0) = 0.1, \hat{\theta}_1(0) = 0, \hat{\theta}_2(0) = 0, \omega_2(0) = 0.1, r(0) = 0.1, \lambda_1(0) = 0, \lambda_2(0) = 0, \zeta_1(0) = 0.1, \zeta_2(0) = 0.1, \Xi_{(1)}(0) = 0, \Xi_{(2)}(0) = 0, \lambda_1(0) = \lambda_2(0) = 0$. The design parameters are selected as follows: $a_1 = a_2 = 1, \sigma_1 = \sigma_2 = 0.001, \tau_2 = 0.25, \gamma_1 = \gamma_2 = 0.001, q = 0.6, n_1 = n_2 = 10, l_1 = l_2 = 10, \beta = 0.3, c_1 = 3.8, c_2 = 2, p = \frac{3}{17}, \hat{b}_m(0) = 3, v_{\min} = 0.2, v_{th} = \frac{v_{10}}{1-\delta}, \delta = \frac{1-p}{1+p}, v_{\min} = p^{1-i} v_{\min}, i = 1, 2, \dots, \infty, k_1 = 15, k_2 = 30$.

The simulation results depicted in Figures 1–4 demonstrate various aspects of the system's performance. Figure 1 shows the actual output y (solid line) closely mirroring the desired trajectory y_d (dotted line), with slight discrepancies indicating the system's capability to approximate the target trajectory effectively. In Figure 2, we compare the original control signal $v(t - \tau)$ (dotted line) against its quantized version $q(v(t - \tau))$ (solid line), where the quantized signal reveals notable abrupt changes, underscoring the effects of quantization. Figure 3 displays the tracking error e_1 , which fluctuates around zero, suggesting competent tracking despite transient peaks. Last, Figure 4 illustrates the raw, unquantized control signal $v(t - \tau)$, characterized by intense fluctuations and spikes, indicative of the system's responsiveness to dynamic changes and corrective actions in real-time.

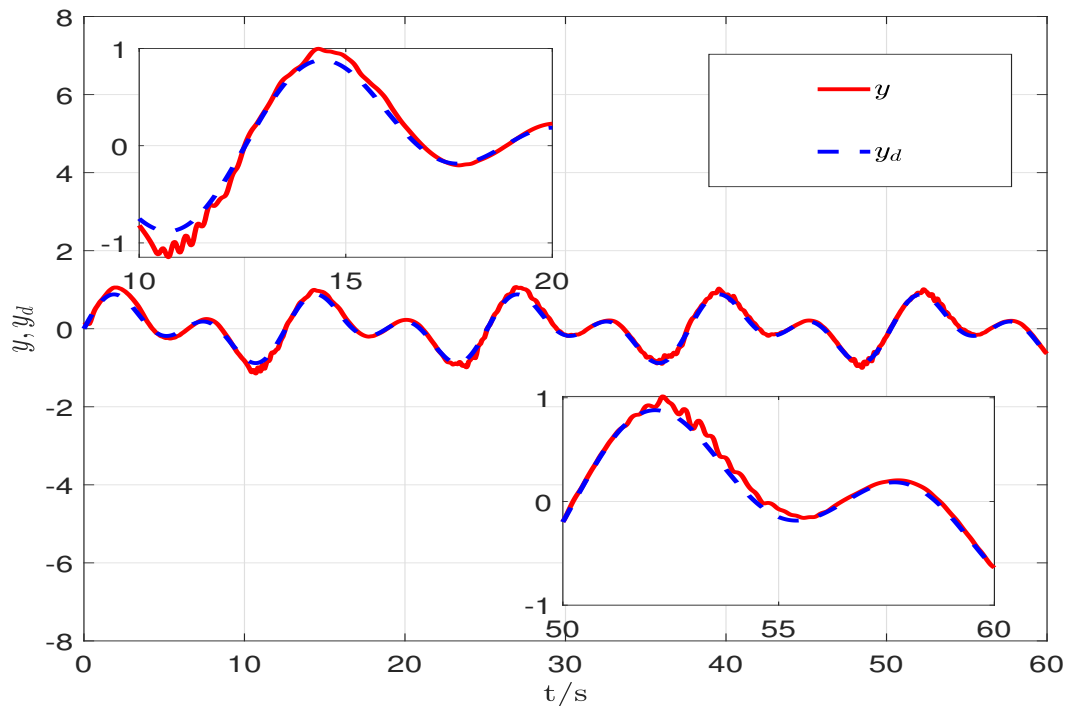


Figure 1. Output y (solid line) and expected trajectory y_d (dotted line).

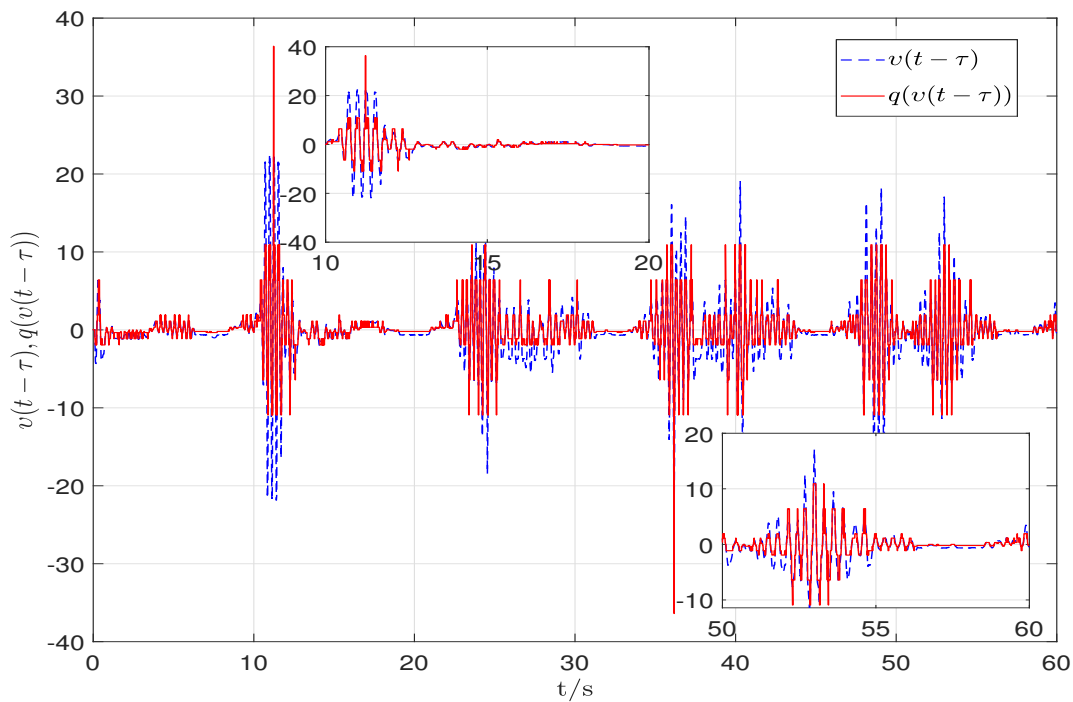


Figure 2. Control signal $v(t - \tau)$ (dotted line) Quantizes control signal $q(v(t - \tau))$ (solid line).

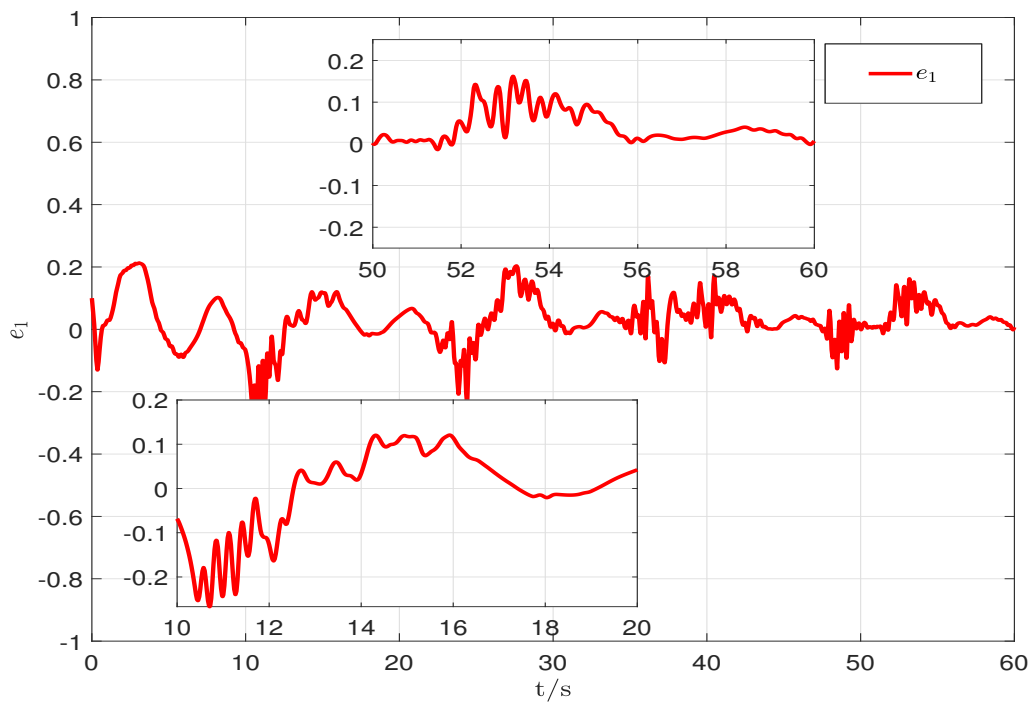


Figure 3. Tracking signal e_1 .

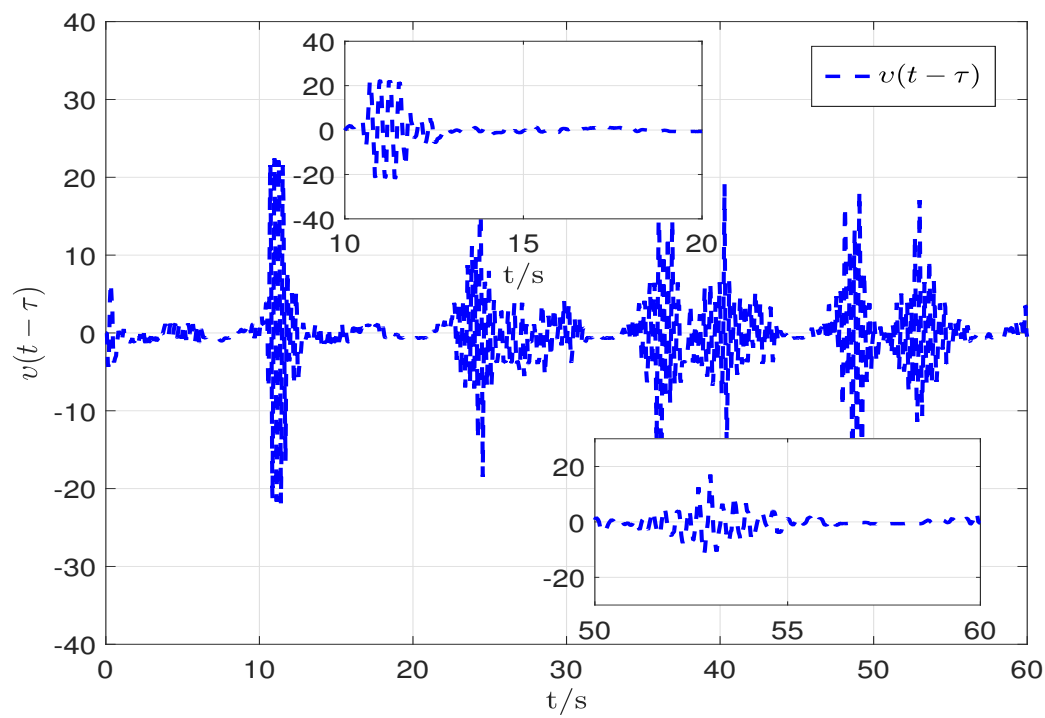


Figure 4. Control signal $v(t - \tau)$.

5. Conclusions

We introduce a novel adaptive dynamic surface control approach designed for nonlinear systems with complex attributes such as unmodeled dynamics, quantized input delays, and dynamic uncertainties. We integrate dynamic signal processing methods to tackle the unmodeled dynamics, thus enhancing the adaptability and robustness of our control strategy. Furthermore, the incorporation of Young's inequality and neural networks into our strategy bolsters its ability to manage inequality constraints and adapt to dynamic uncertainties effectively. An auxiliary function has also been introduced to mitigate the effects of quantized delays, thereby maintaining system performance. Theoretical analysis alongside simulation results affirm that our control strategy ensures all signals remain within bounded limits, showcasing robust control performance amidst complex dynamics. Looking ahead, we plan to extend our research by exploring the integration of more advanced filtering techniques and enhancing the neural network models to increase the control strategy's efficiency and reliability.

Author contributions

Changgui Wu: Conceptualization, Methodology, Investigation, Software, Funding acquisition, Project administration, Supervision, Writing-original draft; Liang Zhao: Conceptualization, Methodology, Software, Writing-review and editing. All authors have read and approved the final version of the manuscript for publication.

Conflict of interest

The authors declare there is no conflict of interest.

References

1. S. D. Gu, J. G. Kuba, Y. P. Chen, Y. L. Du, L. Yang, A. Knoll, et al., Safe multi-agent reinforcement learning for multi-robot control, *Artif. Intell.*, **319** (2023), 103905. <https://doi.org/10.1016/j.artint.2023.103905>
2. Z. B. Liu, K. R. Peng, L. P. Han, S. C. Guan, Modeling and control of robotic manipulators based on artificial neural networks: A review, *Iran. J. Sci. Technol. Trans. Mech. Eng.*, **47** (2023), 1307–1347. <https://doi.org/10.1007/s40997-023-00596-3>
3. K. S. Ratnam, K. Palanisamy, G. Y. Yang, Future low-inertia power systems: Requirements, issues, and solutions-A review, *Renew. Sust. Energ. Rev.*, **124** (2020), 109773. <https://doi.org/10.1016/j.rser.2020.109773>
4. H. Q. Xie, Z. J. Qin, G. Y. Li, B. H. Juang, Deep learning enabled semantic communication systems, *IEEE T. Signal Proces.*, **69** (2021), 2663–2675. <https://doi.org/10.1109/TSP.2021.3071210>
5. M. Hennink, B. N. Kaiser, Sample sizes for saturation in qualitative research: A systematic review of empirical tests, *Soc. Sci. Med.*, **292** (2022), 114523. <https://doi.org/10.1016/j.socscimed.2021.114523>

6. L. You, C. D. Li, X. Y. Zhang, Z. L. He, Edge event-triggered control and state-constraint impulsive consensus for nonlinear multi-agent systems, *AIMS Math.*, **5** (2022), 4151–4167. <https://doi.org/10.3934/math.2020266>
7. D. H. He, B. Z. Bao, L. G. Xu, Robust stability and boundedness of uncertain conformable fractional-order delay systems under input saturation, *AIMS Math.*, **8** (2023), 21123–21137. <https://doi.org/10.3934/math.20231076>
8. X. W. Shao, L. Chen, J. L. Chen, D. X. Zhang, Prescribed-time control for spacecraft formation flying with uncertainties and disturbances, *AIMS Math.*, **9** (2024), 1180–1198. <https://doi.org/10.3934/math.2024058>
9. M. N. A. Parlakci, Robust static output feedback H_∞ controller design for linear parameter-varying time delay systems, *Circuits Syst. Signal Process.*, **43** (2024), 843–864. <https://doi.org/10.1007/s00034-023-02514-z>
10. D. Swaroop, J. K. Hedrick, P. P. Yip, J. C. Gerdes, Dynamic surface control for a class of nonlinear systems, *IEEE T. Automat. Contr.*, **45** (2000), 1893–1899. <https://doi.org/10.1109/TAC.2000.880994>
11. I. Kanellakopoulos, P. V. Kokotovic, A. S. Morse, Systematic design of adaptive controllers for feedback linearizable systems, In: *1991 American Control Conference*, 1991, 649–654. <https://doi.org/10.23919/ACC.1991.4791451>
12. X. F. Wang, M. Y. Sun, A new family of fourth-order Ostrowski-type iterative methods for solving nonlinear systems, *AIMS Math.*, **9** (2024), 10255–10266. <https://doi.org/10.3934/math.2024501>
13. H. Alhazmi, M. Kharrat, Echo state network-based adaptive control for nonstrict-feedback nonlinear systems with input dead-zone and external disturbance, *AIMS Math.*, **9** (2024), 20742–20762. <https://doi.org/10.3934/math.20241008>
14. H. R. Ren, H. Ma, H. Y. Li, R. Q. Lu, A disturbance observer based intelligent control for nonstrict-feedback nonlinear systems, *Sci. China Tech. Sci.*, **66** (2023), 456–467. <https://doi.org/10.1007/s11431-022-2126-7>
15. Q. T. Meng, Q. Ma, Y. Shi, Adaptive fixed-time stabilization for a class of uncertain nonlinear systems, *IEEE T. Automat. Contr.*, **68** (2023), 6929–6936. <https://doi.org/10.1109/TAC.2023.3244151>
16. D. Yang, Y. J. Liu, F. Ding, E. F. Yang, Hierarchical gradient-based iterative parameter estimation algorithms for a nonlinear feedback system based on the hierarchical identification principle, *Circuits Syst. Signal Process.*, **43** (2024), 124–151. <https://doi.org/10.1007/s00034-023-02477-1>
17. J. B. Zhang, F. Ding, Y. Shi, Self-tuning control based on multi-innovation stochastic gradient parameter estimation, *Syst. Control Lett.*, **58** (2009), 69–75. <https://doi.org/10.1016/j.sysconle.2008.08.005>
18. Y. Sun, M. Chen, C. Gao, L. B. Wu, Output feedback command filtered fuzzy controller design for uncertain strict-feedback nonlinear systems with unmodeled dynamics and event-triggered strategy, *Eng. Res. Express*, **6** (2024), 025315. <https://doi.org/10.1088/2631-8695/ad3f75>
19. G. Q. Ma, P. R. Pagilla, Periodic event-triggered dynamic output feedback control of switched systems, *Nonlinear Anal-Hybri.*, **31** (2019), 247–264. <https://doi.org/10.1016/j.nahs.2018.10.001>

20. X. N. Xia, T. P. Zhang, Adaptive output feedback dynamic surface control of nonlinear systems with unmodeled dynamics and unknown high-frequency gain sign, *Neurocomput.*, **143** (2014), 312–321. <https://doi.org/10.1016/j.neucom.2014.05.061>
21. T. P. Zhang, M. Z. Xia, J. M. Zhu, Adaptive backstepping neural control of state-delayed nonlinear systems with full-state constraints and unmodeled dynamics, *Int. J. Adapt. Control Signal Process.*, **31** (2017), 1704–1722. <https://doi.org/10.1002/acs.2795>
22. T. P. Zhang, X. N. Xia, Decentralized adaptive fuzzy output feedback control of stochastic nonlinear large-scale systems with dynamic uncertainties, *Inform. Sci.*, **315** (2015), 17–38. <https://doi.org/10.1016/j.ins.2015.04.002>
23. L. Xu, F. Ding, X. Zhang, Q. M. Zhu, Novel parameter estimation method for the systems with colored noises by using the filtering identification idea, *Syst. Control Lett.*, **186** (2024), 105774. <https://doi.org/10.1016/j.sysconle.2024.105774>
24. L. T. Xing, C. Y. Wen, Y. Zhu, H. Y. Su, Z. T. Liu, Output feedback control for uncertain nonlinear systems with input quantization, *Automatica*, **65** (2016), 191–202. <https://doi.org/10.1016/j.automatica.2015.11.028>
25. K. Yu, X. H. Chang, Quantized output feedback resilient control of uncertain systems under hybrid cyber attacks, *Int. J. Adapt. Control Signal Process.*, **36** (2022), 2954–2970. <https://doi.org/10.1002/acs.3496>
26. N. Li, J. Feng, Quantized feedback adaptive reliable H_∞ control for linear time-varying delayed systems, *Circuits Syst. Signal Process.*, **35** (2016), 851–874. <https://doi.org/10.1007/s00034-015-0109-2>
27. Y. X. Li, G. H. Yang, Adaptive asymptotic tracking control of uncertain nonlinear systems with input quantization and actuator faults, *Automatica*, **72** (2016), 177–185. <https://doi.org/10.1016/j.automatica.2016.06.008>
28. T. F. Liu, Z. P. Jiang, D. J. Hill, A sector bound approach to feedback control of nonlinear systems with state quantization, *Automatica*, **48** (2012), 142–152. <https://doi.org/10.1016/j.automatica.2011.09.041>
29. W. L. Chen, J. H. Wang, K. M. Ma, T. Wang, Adaptive event-triggered neural control for nonlinear uncertain system with input constraint, *Int. J. Robust Nonlin.*, **30** (2020), 3801–3815. <https://doi.org/10.1002/rnc.4965>
30. J. L. Ma, S. Y. Xu, Y. M. Li, Y. M. Chu, Z. Q. Zhang, Neural networks-based adaptive output feedback control for a class of uncertain nonlinear systems with input delay and disturbances, *J. Franklin I.*, **355** (2018), 5503–5519. <https://doi.org/10.1016/j.jfranklin.2018.05.045>
31. T. P. Zhang, X. N. Xia, J. M. Zhu, Adaptive neural control of state delayed nonlinear systems with unmodeled dynamics and distributed time-varying delays, *IET Control Theory Appl.*, **8** (2014), 1071–1082. <https://doi.org/10.1049/iet-cta.2013.0803>
32. Q. Zhu, S. M. Fei, T. P. Zhang, T. Li, Adaptive RBF neural-networks control for a class of time-delay nonlinear systems, *Neurocomput.*, **71** (2008), 3617–3624. <https://doi.org/10.1016/j.neucom.2008.04.012>
33. L. D. Fang, L. Ma, S. H. Ding, Finite-time fuzzy output-feedback control for p-norm stochastic nonlinear systems with output constraints, *AIMS Math.*, **6** (2021), 2244–2267. <https://doi.org/10.3934/math.2021136>

34. A. L. Li, X. L. Ye, Finite-time anti-synchronization for delayed inertial neural networks via the fractional and polynomial controllers of time variable, *AIMS Math.*, **6** (2021), 8173–8190. <https://doi.org/10.3934/math.2021473>
35. S. P. Bhat, D. S. Bernstein, Finite-time stability of continuous autonomous systems, *SIAM J. Control Optim.*, **38** (2000), 751–766. <https://doi.org/10.1137/S0363012997321358>
36. Y. M. Li, K. W. Li, S. C. Tong, Finite-time adaptive fuzzy output feedback dynamic surface control for MIMO nonstrict feedback systems, *IEEE T. Fuzzy Syst.*, **27** (2019), 96–110. <https://doi.org/10.1109/TFUZZ.2018.2868898>
37. C. X. Wang, J. L. Du, J. B. Yu, Adaptive finite-time tracking control for time-varying output constrained nonlinear systems with unmatched uncertainties, *IET Control Theory Appl.*, **13** (2019), 2416–2424. <https://doi.org/10.1049/iet-cta.2018.5458>
38. Y. Zhang, F. Wang, J. Zhang, Adaptive finite-time tracking control for output-constrained nonlinear systems with non-strict-feedback structure, *Int. J. Adapt. Control Signal Process.*, **34** (2020), 560–574. <https://doi.org/10.1002/acs.3099>
39. J. P. Li, Y. Yang, C. C. Hua, X. P. Guan, Fixed-time backstepping control design for high-order strict-feedback nonlinear systems via terminal sliding mode, *IET Control Theory Appl.*, **11** (2017), 1184–1193. <https://doi.org/10.1049/iet-cta.2016.1143>
40. Y. Hua, T. P. Zhang, Adaptive finite-time optimal fuzzy control for novel constrained uncertain nonstrict feedback mixed multiagent systems via modified dynamic surface control, *Inform. Sci.*, **681** (2024), 121216. <https://doi.org/10.1016/j.ins.2024.121216>
41. Y. X. Li, Finite time command filtered adaptive fault tolerant control for a class of uncertain nonlinear systems, *Automatica*, **106** (2019), 117–123. <https://doi.org/10.1016/j.automatica.2019.04.022>
42. H. J. Brascamp, E. H. Lieb, Best constants in Young's inequality, its converse, and its generalization to more than three functions, *Adv. Math.*, **20** (1976), 151–173. [https://doi.org/10.1016/0001-8708\(76\)90184-5](https://doi.org/10.1016/0001-8708(76)90184-5)
43. S. Y. Gao, F. S. Li, H. Wang, Evaluation of the effects of oxygen enrichment on combustion stability of biodiesel through a PSO-EMD-RBF model: An experimental study, *AIMS Math.*, **9** (2024), 4844–4862. <https://doi.org/10.3934/math.2024235>
44. H. H. Qiu, L. Wan, Z. G. Zhou, Q. J. Zhang, Q. H. Zhou, Global exponential periodicity of nonlinear neural networks with multiple time-varying delays, *AIMS Math.*, **8** (2023), 12472–12485. <https://doi.org/10.3934/math.2023626>
45. Y. Linde, A. Buzo, R. Gray, An algorithm for vector quantizer design, *IEEE T. Commun.*, **28** (1980), 84–95. <https://doi.org/10.1109/TCOM.1980.1094577>
46. Y. F. Sun, L. L. Li, D. W. C. Ho, Quantized synchronization control of networked nonlinear systems: Dynamic quantizer design with event-triggered mechanism, *IEEE T. Cybernetics*, **53** (2023), 184–196. <https://doi.org/10.1109/TCYB.2021.3090999>

